Exploring High-z Universe with Subaru/GLAO and TMT

Masayuki Akiyama (Tohoku Univ.)
Ikuru Iwata (Subaru Telescope)

Inprint of the “galaxy formation”

- Recent observations suggests re-ionization of the universe happened in between z~10 and 6. The era of re-ionization should be connected to the initial phase of galaxy formation.

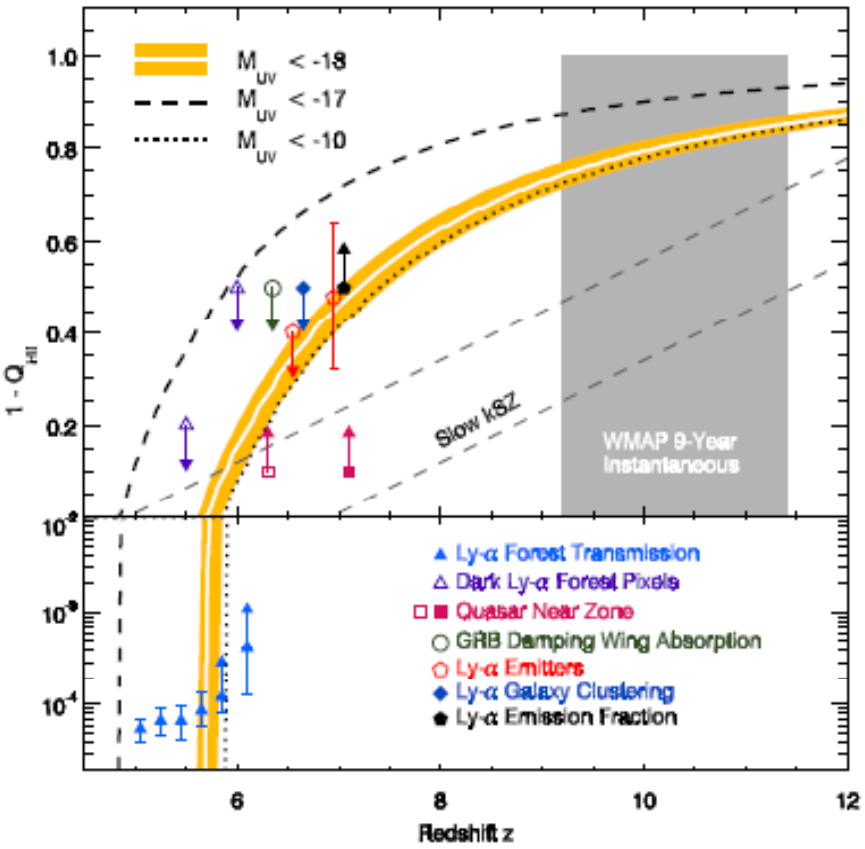

Robertson et al. 2013, ApJ, 768, 71

Age of the universe: 8.3e+8@z~6, 5.4e+8@z~8, 3.8e+8@z~10

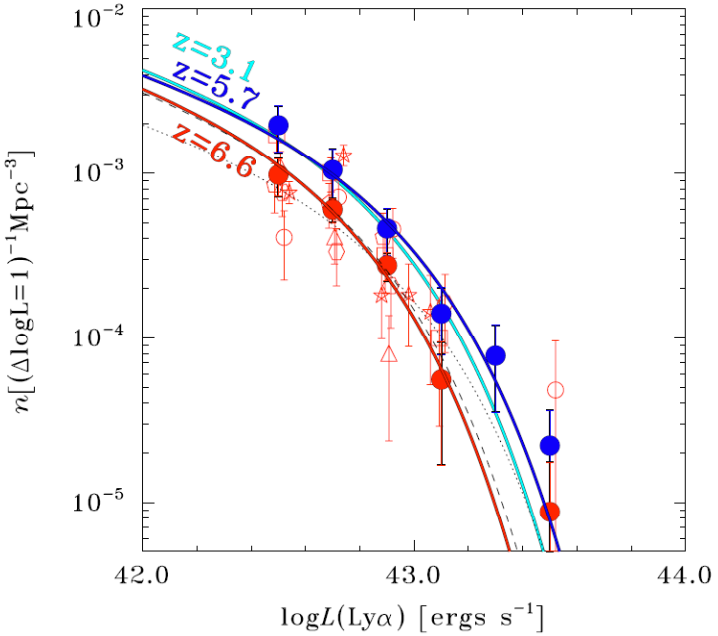

Ouchi et al. 2010, ApJ, 723, 869

Young galaxies at high-z

- Rest-frame UV-selected (Lyman break) galaxies at z~5 are on average younger than UV-selected galaxies at z~2-3. The observed starformation time scale (age and Mstar/SFR) is comparable to the age of the universe at z~6-10.

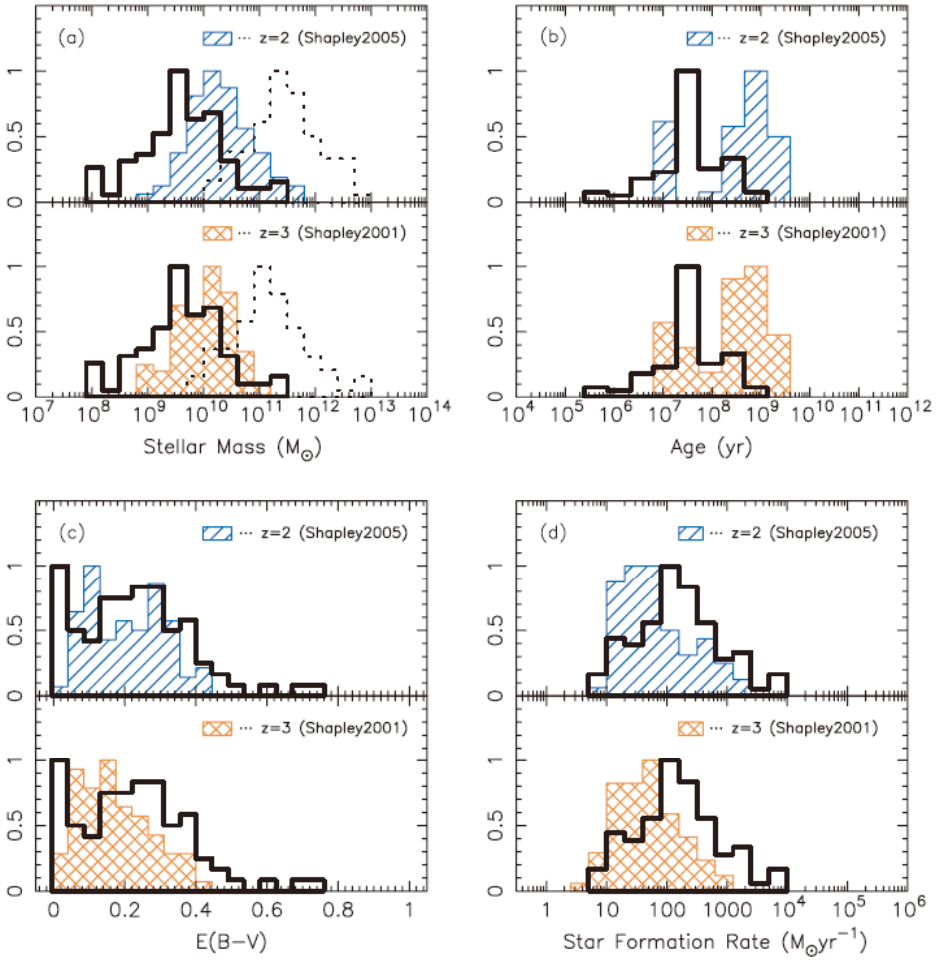

Yabe et al. 2009, ApJ, 693, 507
Age of the universe: 3e+9@z~2, 2e+9@z~3, 1e+9@z~5

Outline of my talk

1. TMT for galaxies at z~6-10
   - Observations in 2020s :
     - ALMA : molecular gas and dust properties
     - JWST(2018-) : rest-frame optical properties
     - TMT(2021-) : rest-frame UV properties

     - Condition of star-formation in the early universe

2. Subaru GLAO NIR imager for finding LAEs at z~6-10
   - Consider Subaru/GLAO as a supplier of targets

TMT for galaxies at z~6-10

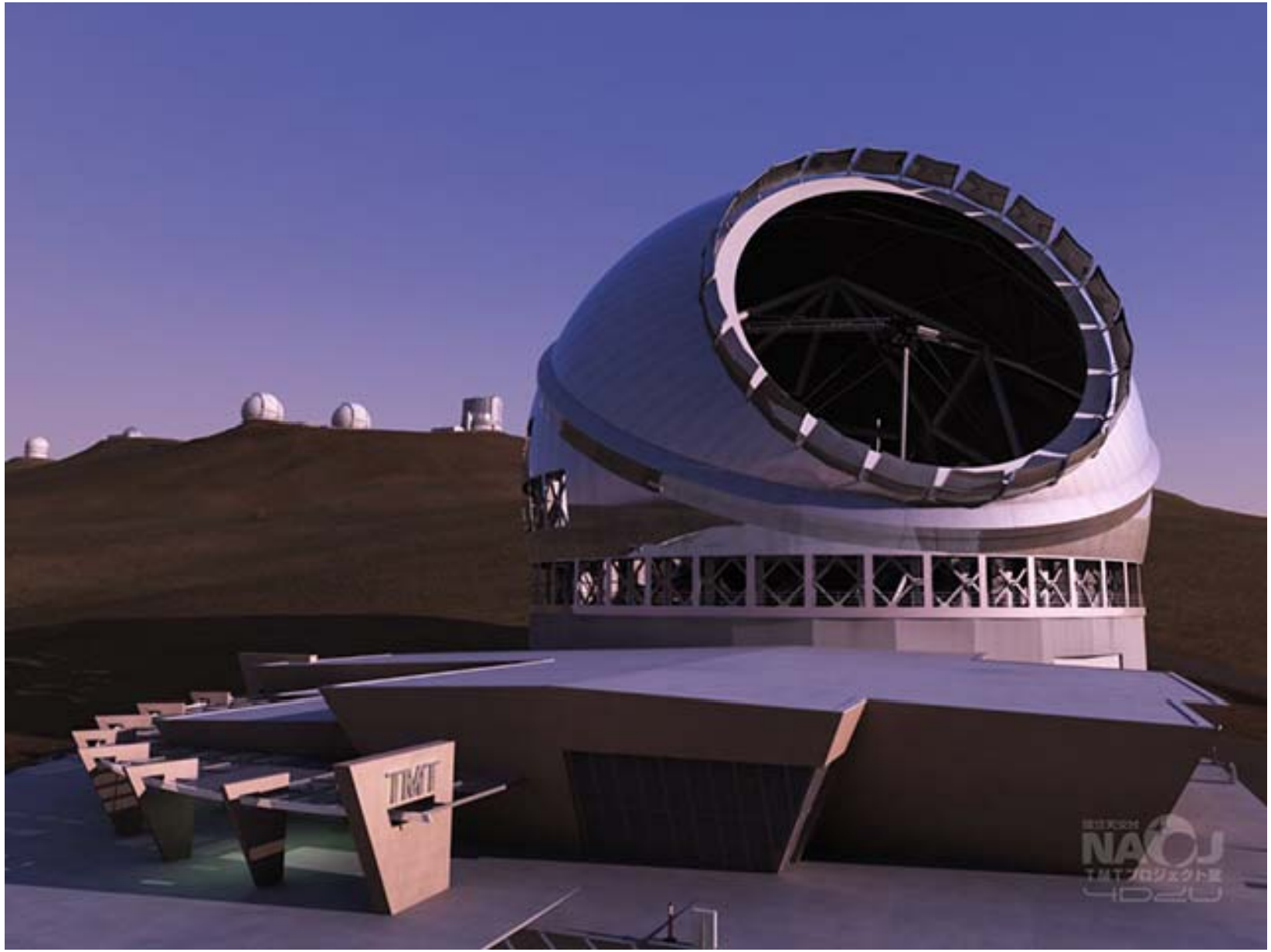

TMT for galaxies at z~6-10

Early light = First generation instruments

- IRIS: Near-infrared IFU + imager supported by the best AO correction (MCAO)
  - 0.45″x0.64″ 0.004″ sampling with R~4,000
  - 2.25″x4.5″ 0.050″ sampling with R~4,000
  - 17″ x 17″ fov for imaging with 0.004″ sampling
- IRMS: Near-infrared Multi-Object Spectrograph supported by moderate AO correction (MCAO in wide-field)
  - 2′x2′ Multi-Slit with R~4,000

Candidates of next generation instruments

- IRMOS: Multiple Near-infrared IFUs (~20) with good AO correction (MOAO)
  - 5′ diameter fov
- NIRES: Near infrared high-resolution spectrograph with MCAO
  - R>20,000

- TMT-AGE (Analyzer for Galaxies in the Early universe: J-IRMOS) with MOAO
  - IRMOS-like instruments with wider FoV, possibly ~10′ diameter

AO is the key component to maximize the capabilities of the NIR instruments.

TMT for galaxies at z~6-10 : rest-frame UV spectrum

Contains rich information on young stars in the young galaxies.

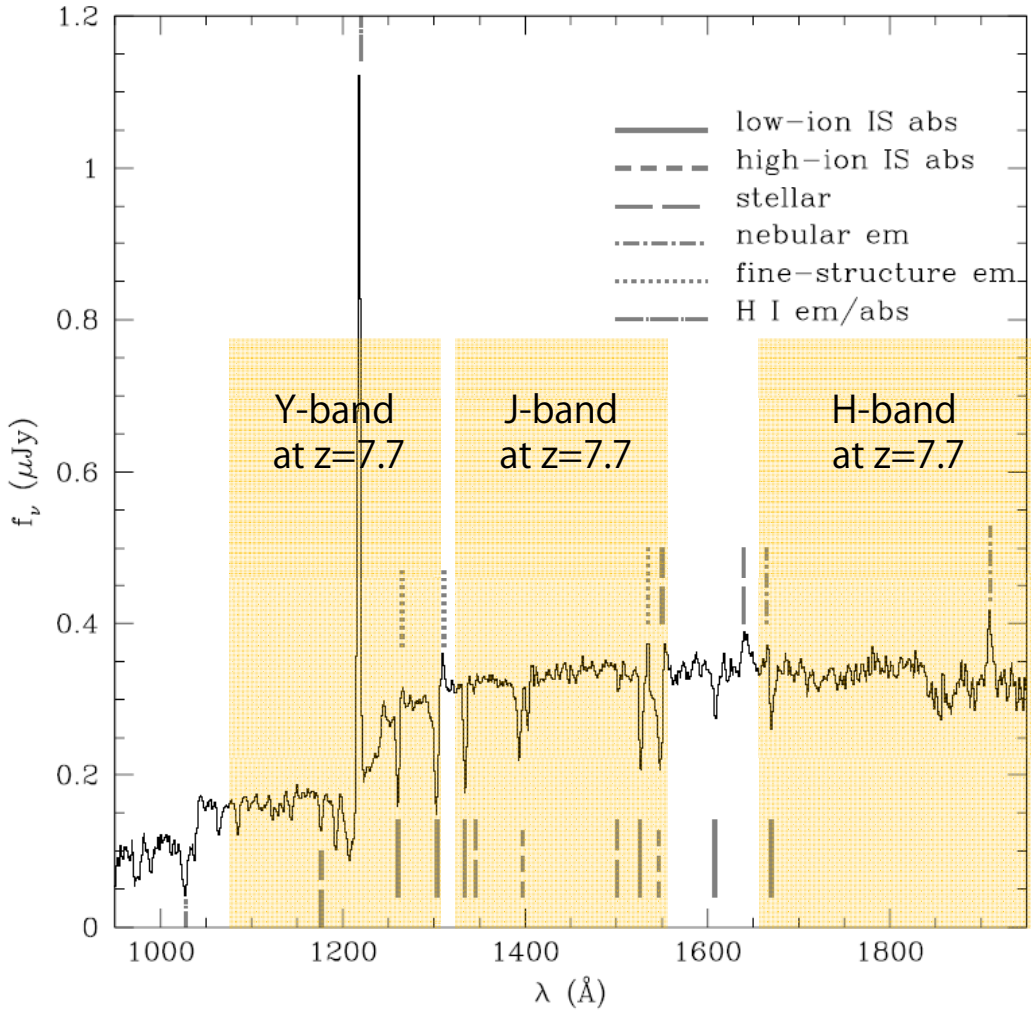

Shapley et al. 2003, ApJ, 588, 65

Lya:1216

CIII:1176 (Ste)
OIV: 1343 (Ste)
SV:1501 (Ste)
HeII:1640 (Ste)

SiII:1260 (LI)
SiII:1265 (em)
OI+SiII:1303 (LI)
SiII:1309 (em)
CII:1334 (LI)
SiII:1526 (LI)
SiII:1533 (em)
FeII:1608 (LI)
AlII:1670 (LI)

SiIV:1393
SiIV:1402
CIV:1549
OIII]:1663
OIII] :1661 (em)
OIII]:1666 (em)
CIII]:1907,1909 (em)

Signitures of massive stars and dependence on IMF shape

Profiles of CIV 1549 and SiIV 1400 lines depend on the IMF slope: contribution from stars with P-Cyg profile

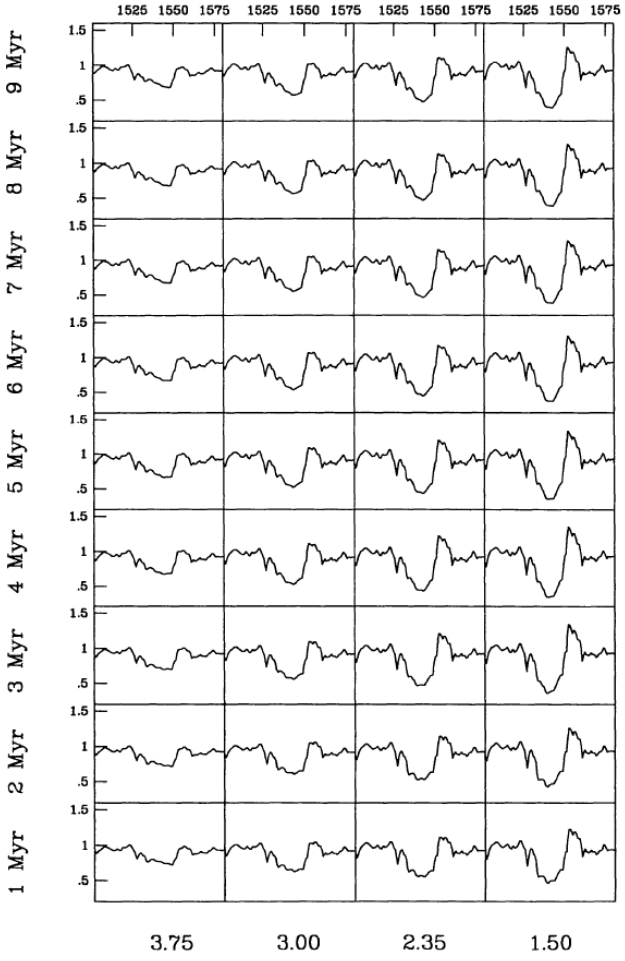

FIG. 4.—Same as Fig. 2, but for continuous star formation

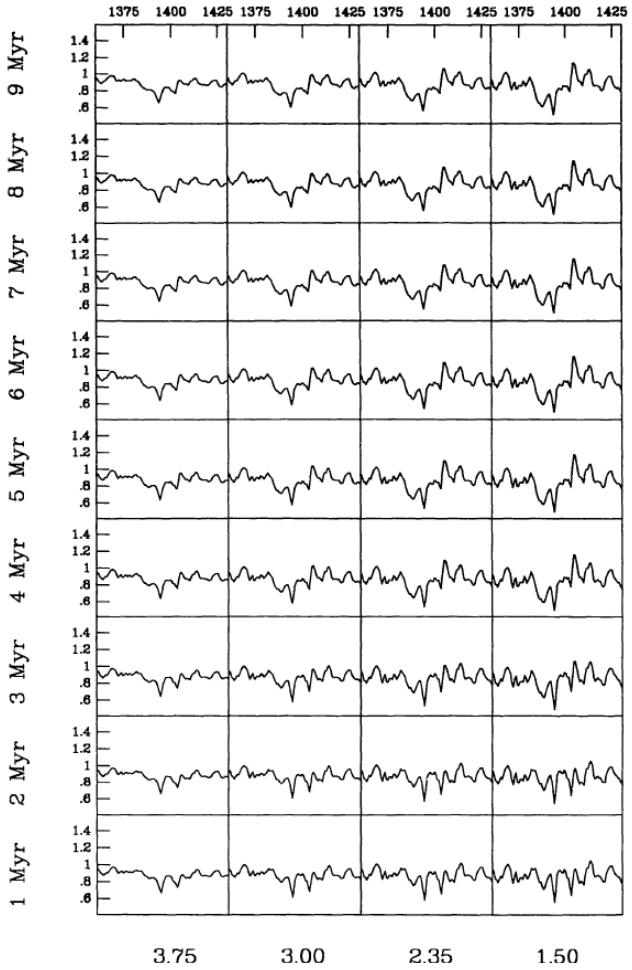

FIG. 8.—Same as Fig. 4, but for Si IV λ1400

Leitherer et al. ApJS, 1995, 99, 173

Signitures of outflow of low-ionization gas

Velocity offset of UV inter-stellar lines and Ly-a line from nebular emission lines represent large scale gas dynamics of galaxies.

Observed velocity offsets for z~2 galaxies:

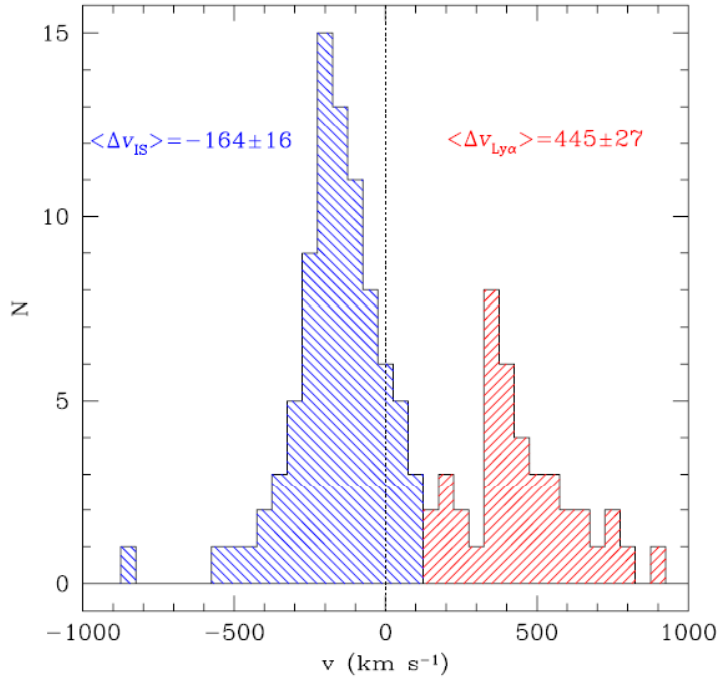

Figure 1. Histogram of the measured (centroid) velocities of IS absorption lines (blue) and Lyα emission (red) with respect to the galaxy nebular redshift as defined by the centroid of the Hα emission line, for a sample of 89 galaxies with $\langle z \rangle = 2.27 \pm 0.16$. The sample includes only those galaxies having both nebular line redshifts and rest-UV spectra of adequate quality to measure absorption line centroids. In this sample, 86 of the 89 galaxies have measured values of $z_{\rm IS}$, 3 have only $z_{\rm Ly\alpha}$, and 39 have both. The mean values of the velocity offsets are indicated.

Steidel et al. ApJ, 717, 289

Signatures of re-ionization

Damped profile of Ly-a absorption line reflects the existence of neutral IGM in front of the galaxies (solid line).

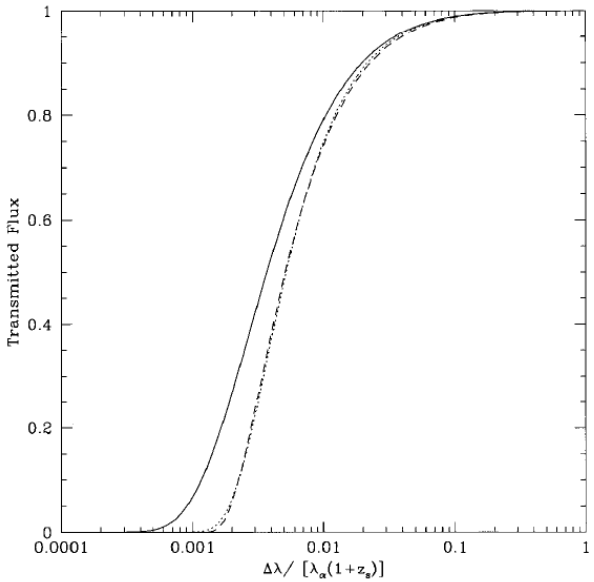

FIG. 1.—Absorption profile of the damping wing of the Gunn-Peterson trough, predicted using the equation given in the Appendix. The fraction of transmitted flux is shown as a function of the wavelength interval $\Delta\lambda$ from the Lyα wavelength of the source, $\lambda_\alpha(1 + z_s)$. The solid line assumes the parameters $z_s = 9$, $\tau_0 = 4.3 \times 10^5$, and $z_n = 7$ (where the IGM is assumed to have a constant neutral density at $z_n < z < z_s$, and be fully ionized at $z < z_n$). The dotted line is the case where an absorption system with $N_{\rm H\,I} = 2 \times 10^{20}$ cm^{-2} is present at $z_s = 9$, which could be due to a galaxy where the source is located. The dashed line shows the damping wing profile without any additional absorption system, but with the parameters changed to $z_s = 9.009$ (although $\Delta\lambda$ is still defined as the wavelength interval from the Lyα line at $z = 9$), $\tau_0 = 4.9 \times 10^5$, and provides the best fit to the dotted line, assuming there is no absorption system at the source redshift. This illustrates the difficulty in measuring τ_0 in the presence of an absorption system.

Miralda-Escude 1998, ApJ, 501, 15

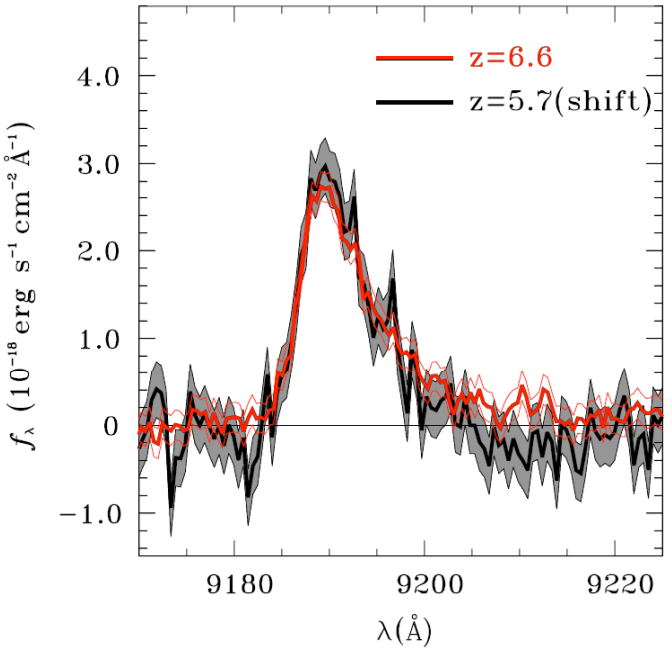

Figure 17. Evolution of LAE spectra. Red and black thick lines represent composite spectra of LAEs at $z = 6.6$ and 5.7, respectively. For comparison of line shapes, the composite spectrum of the $z = 5.7$ LAEs is redshifted to $z = 6.6$, and scaled by an arbitrary factor. 1σ errors of the composite spectra are shown with thin red lines for $z = 6.6$ LAEs and a gray shade for $z = 5.7$ LAEs.

Ouchi et al. 2010, ApJ, 723, 869

Frontier of Subaru (related) studies

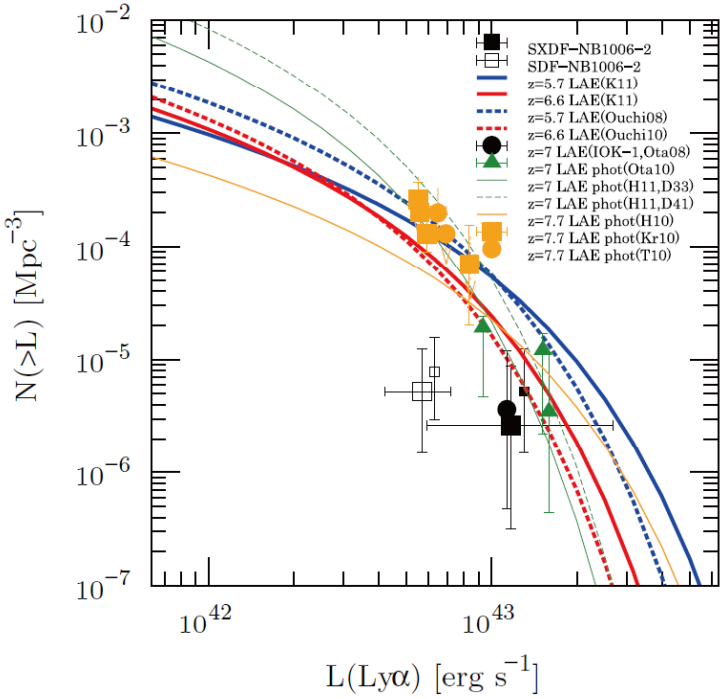

z=7.3 LAE
Subaru Scam(red-sensitive CCD)
NB1006, 22h exp.
FWHM 0.98”
24.83mag (5sigma)
(Shibuya et al. 2012)

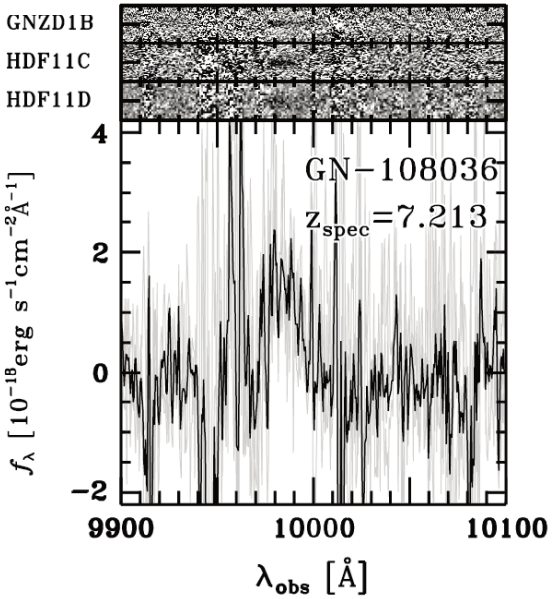

Figure 2. Spectrum of the $z = 7.213$ z-dropout galaxy, GN-108036. The top panels show its two-dimensional spectra obtained with the GNZD1B, HDF11C, and HDF11D masks. The size along the spatial axis is 5.″0 for each two-dimensional spectrum. The HDF11D spectrum is binned in 2×2 pixels. A line is visually identified at $\simeq$9980 Å in the spectra of GNZD1B and HDF11C, whose exposure times are 5 hr and $\simeq$4 hr, respectively, while the line is marginally seen in the spectrum of HDF11D, whose exposure time is 2 hr. In the bottom panel, we show the one-dimensional spectra. The gray solid lines are spectra obtained with individual masks. The composite spectrum is shown as the black solid line. All the one-dimensional spectra illustrate a line detection at around 9980 Å, and the S/N of the line in the composite spectrum is $\simeq$6.

z=7.2 LBG
Keck DEIMOS, 11h exp.
fLya=2.5e-17 erg/s/cm2
Llya=1.5e+43 erg/s
(Ono et al. 2012)

Current observational limit on Lyα LF at z=7.7

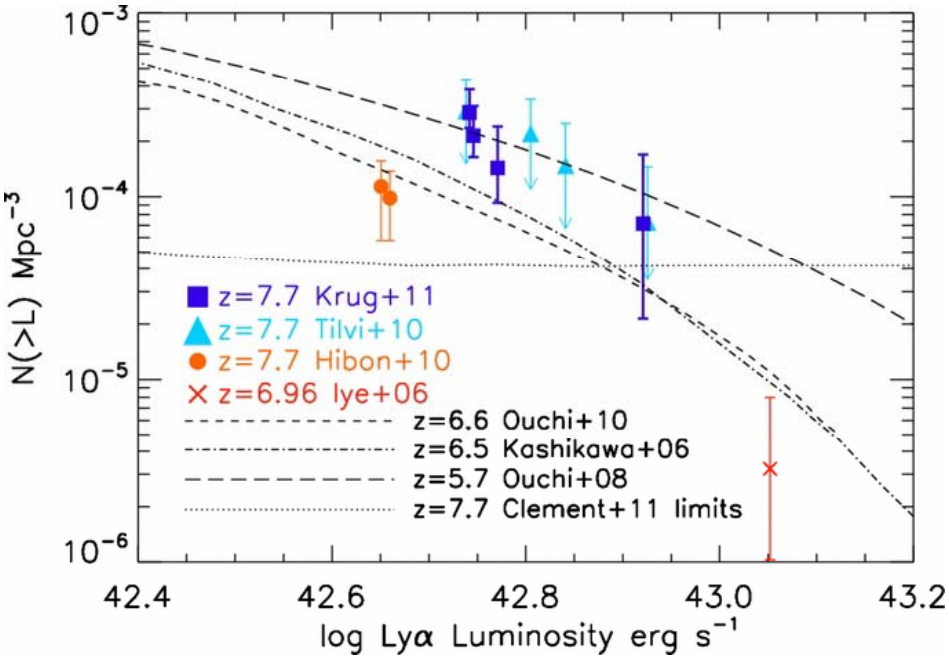

Krug et al. 2012 ApJ 745:122
Clements et al. 2012, A&A 538, A66

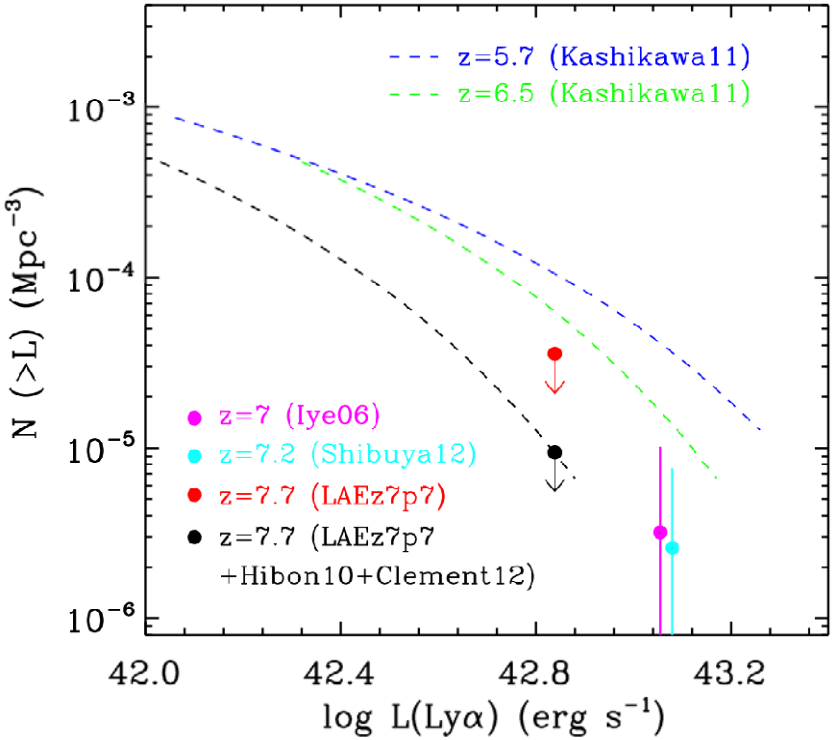

Jiang et al. arXiv:1305.5257

Ultra NB observation with Mayall 4m/NEWFIRM (Krug et al.) vs. NB observation with VLT/Hawk-I (Clements et al.). The brightest emission line candidates found in NEWFIRM survey is not confirmed with LBT spectroscopy.

TMT capabilities

- TMT detection limit for Lya emission line

  With IRIS 1e-18 erg/s/cm2 (SN=10, 5 hours, 0.1" extended with 0.05" sampling, Wright and Barton, 2010, SPIE)

  Log L_Lya = 41.85 erg/s at z=7.7

  Log L_Lya = 42.11 erg/s at z=10.0

TMT capabilities

- Detection limit for UV continuum emission with moderate resolution spectroscopy (ex. binning R~3,000 spectrum to R~500)

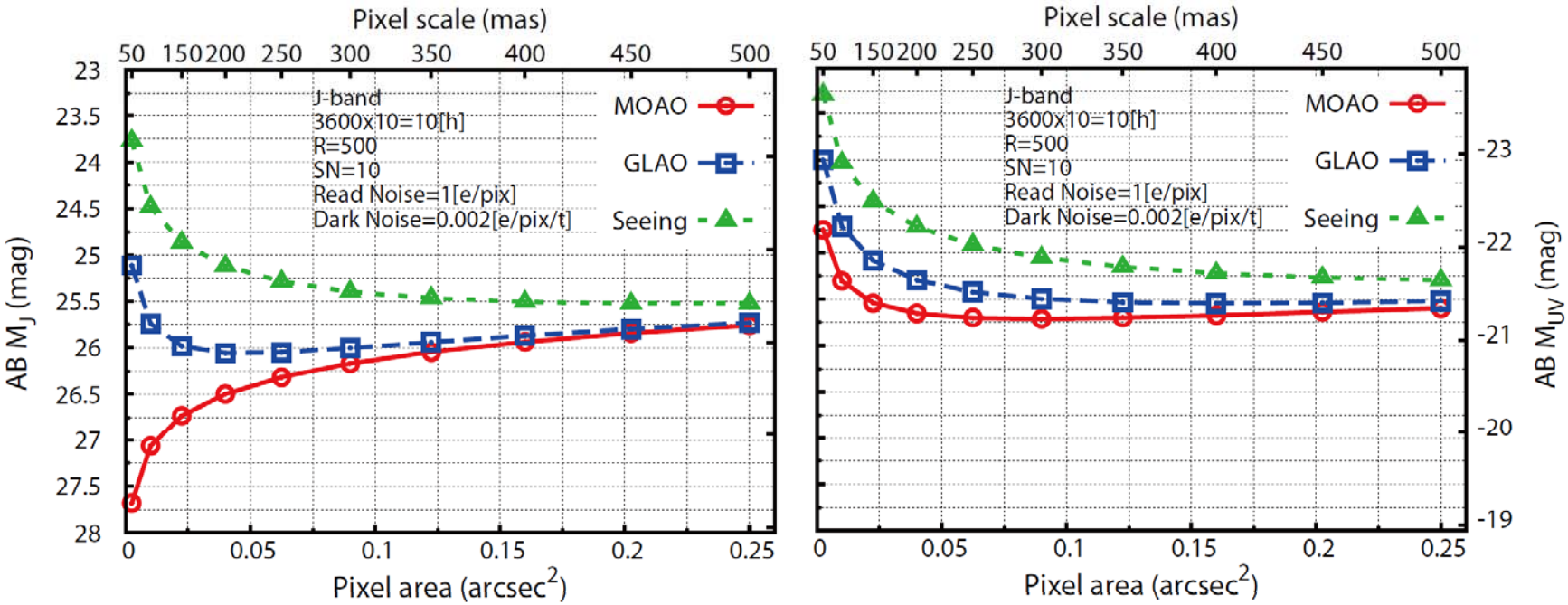

By Yoshito Ono

<u>Galaxies at z~6 is still significantly extended (extended with re~0.125).</u>
<u>J-band continuum limit ~ 25.75 AB magnitude</u>

TMT capabilities

- Number density of z~6-7 galaxies with bright UV continuum is not so high.
- 5objects per fov is the dot-dashed lines.

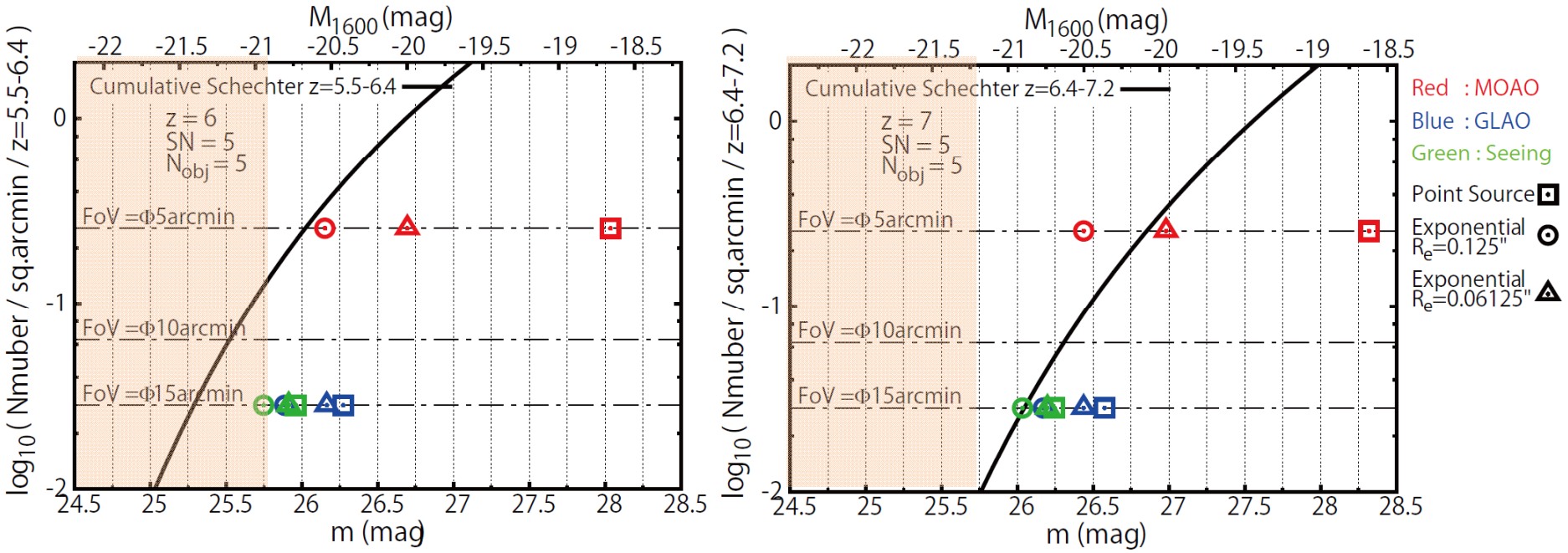

By Yoshito Ono

Outline of my talk

1. TMT for galaxies at z~6-10
   - Observations in 2020s :
     - ALMA : molecular gas and dust properties
     - JWST(2018-) : rest-frame optical properties
     - TMT(2021-) : rest-frame UV properties

     - Condition of star-formation in the early universe

2. Subaru GLAO NIR imager for finding LAEs at z~6-10
   - Consider Subaru/GLAO as a supplier of targets

Capabilities and competitiveness of Subaru + GLAO: Broad-band sensitivity comparison (10,000s exposure, 5sigma, AB)

For broad-band imaging, observation from space can achieve much deeper flux limit thanks to low-background level or no OH line. (Ground-based observations have advantage in the size of FoV.)

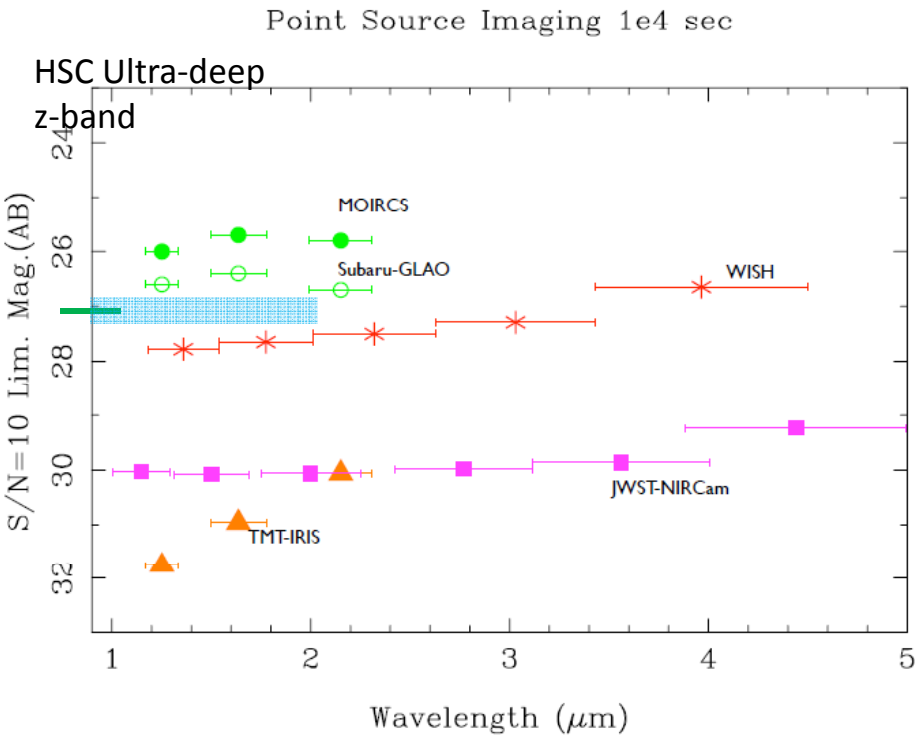

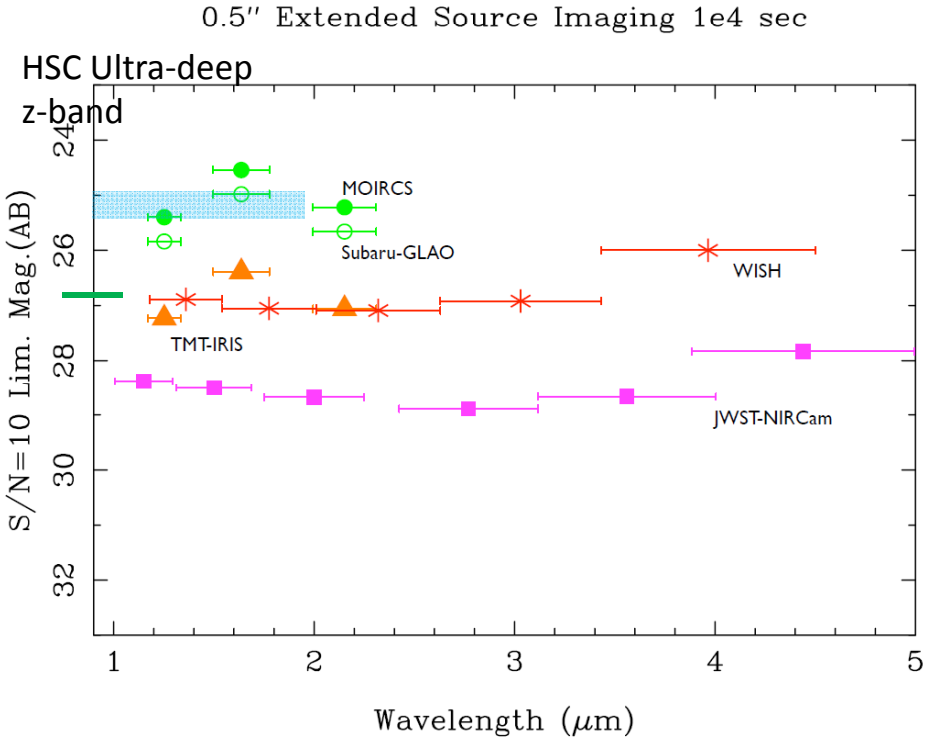

Cyan hatch : TMT continuum spec. limit

By I.Iwata

Comparison with “other” wide field NIR missions in 2020s

- Euclid : 0.6” sampling
- WFIRST-2.4 : 2,000 sq.deg survey with 0.281 sq.deg FoV
- Both of them covers below 2.0um.

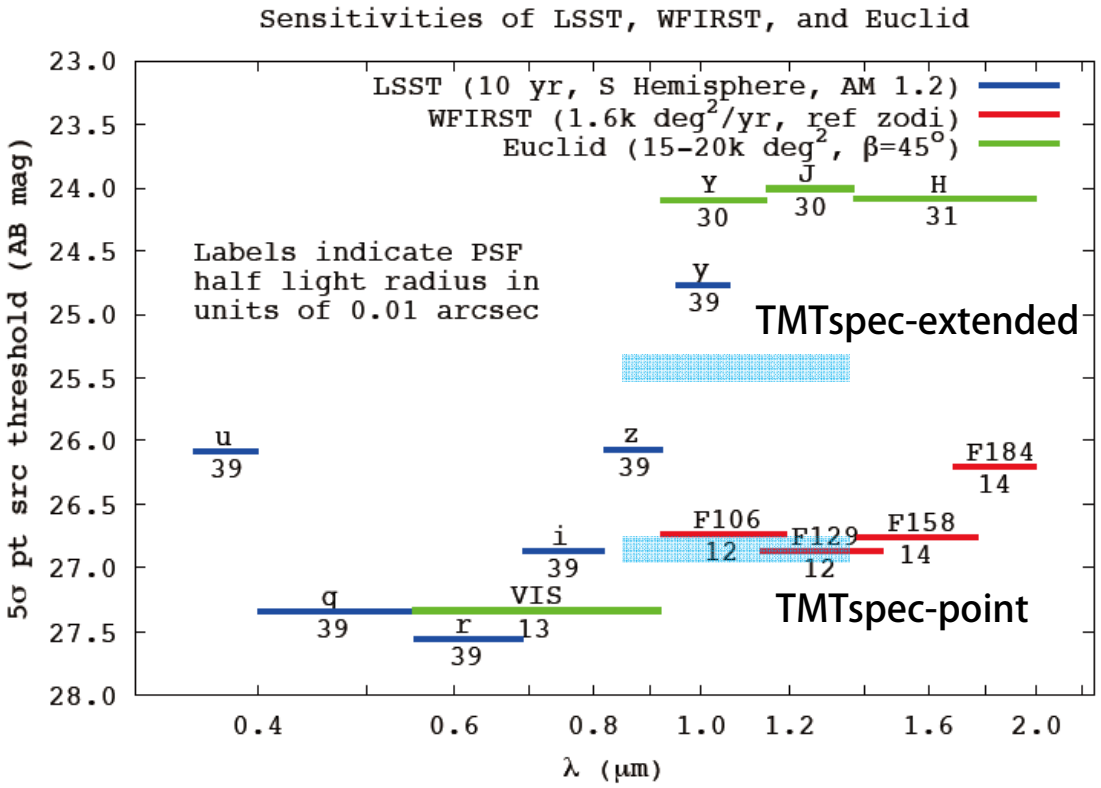

Spergel et al. 2013

Lower and upper cyan hatches represent TMT continuum spectroscopy limits for point and extended (re=0.2”) sources, respectively.

Figure 2: Depth of the WFIRST-2.4 high-latitude imaging survey (red), expressed in AB magnitudes for a 5σ point source detection, compared to the expected depth of the Euclid (green) and LSST (blue) imaging surveys. Labels below each bar indicate the size of the PSF (specifically, the EE50 radius) in units of 0.01 arcsec. The near-IR depth of the the WFIRST-2.4 HLS is well matched to the optical depth of LSST (10-year co-add).

Narrow-band calculations by Iwata

	Mirror [m]	Pix scale ["/pix]	FoV [arcmin2]
Subaru / MOIRCS	8.2m	0.117	28
Subaru / GLAO+WFI	8.2m	0.117	177
JWST / NIRCam	6.5m	0.0317	9.68
WISH	1.5m	0.155	840

For Subaru GLAO+WFI, three narrow band filters are assumed,

NB106 10600A with top-hat filter with d=150A targetting LAEs @ z=7.7

Co-moving volume: 5.0e+3 Mpc^3 / fov

NB134 13400A with top-hat filter with d=190A targetting LAEs @ z=10.0

Co-moving volume: 4.0e+3 Mpc^3 / fov

NB155 15500A with top-hat filter with d=220A targetting LAEs @ z=11.8

Co-moving volume: 3.4e+3 Mpc^3 / fov

JWST has narrow-band filter only above 16000A, can conduct slit-less low-res spectroscopy with NIRISS

NBF transmissions, Atmospheric transmission and Skylines

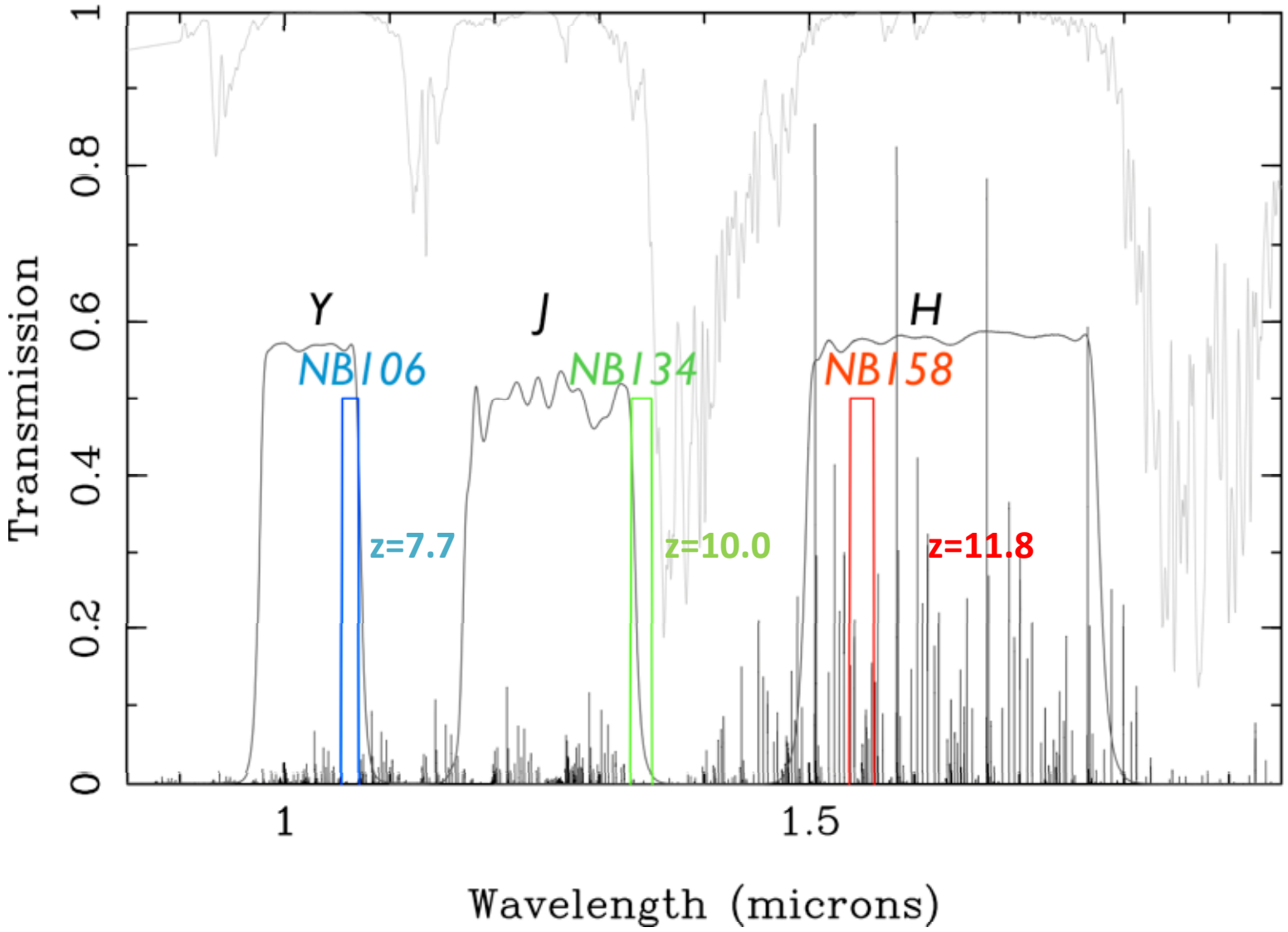

Narrow-band filter detection limit (10h exposure, 10sigma, AB)

If narrow-band observation in between strong OH lines is assumed, ground-based observation can reach similar depth to the observation from space. So continuum selections (like dropout) is better from space, but line selections (like Ly-alpha emitter) can be done efficiently from ground.

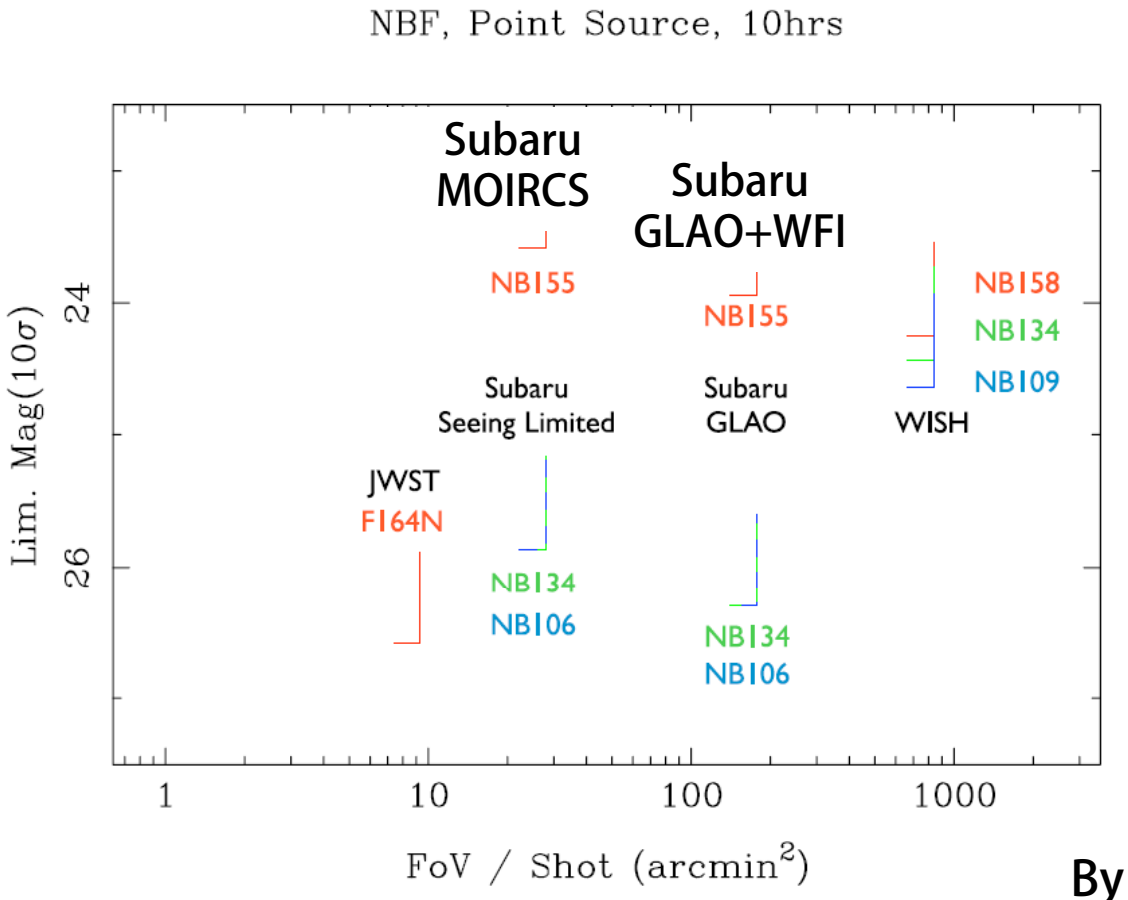

By I.Iwata

Comparison with JWST NIRISS slitless spectroscopy

Instruments	5σ Emission Line Detection Limit (10 hrs)
Subaru Seeing Limited	3.5e-18
Subaru GLAO	2.3e-18
JWST NIRISS (Slitless Spec.)	2.6e-18

For LAE at z~7.7.
Units are erg/s/cm^2.
Note: Sky background assumed for Subaru may be too optimistic.

- JWST NIRCam does not have NBF $\lambda < 1.6\,\mu$m
- JWST NIRISS: R~150 Slitless spectroscopy with 2.2'x2.2' FoV

Detection limit with 10h exp.

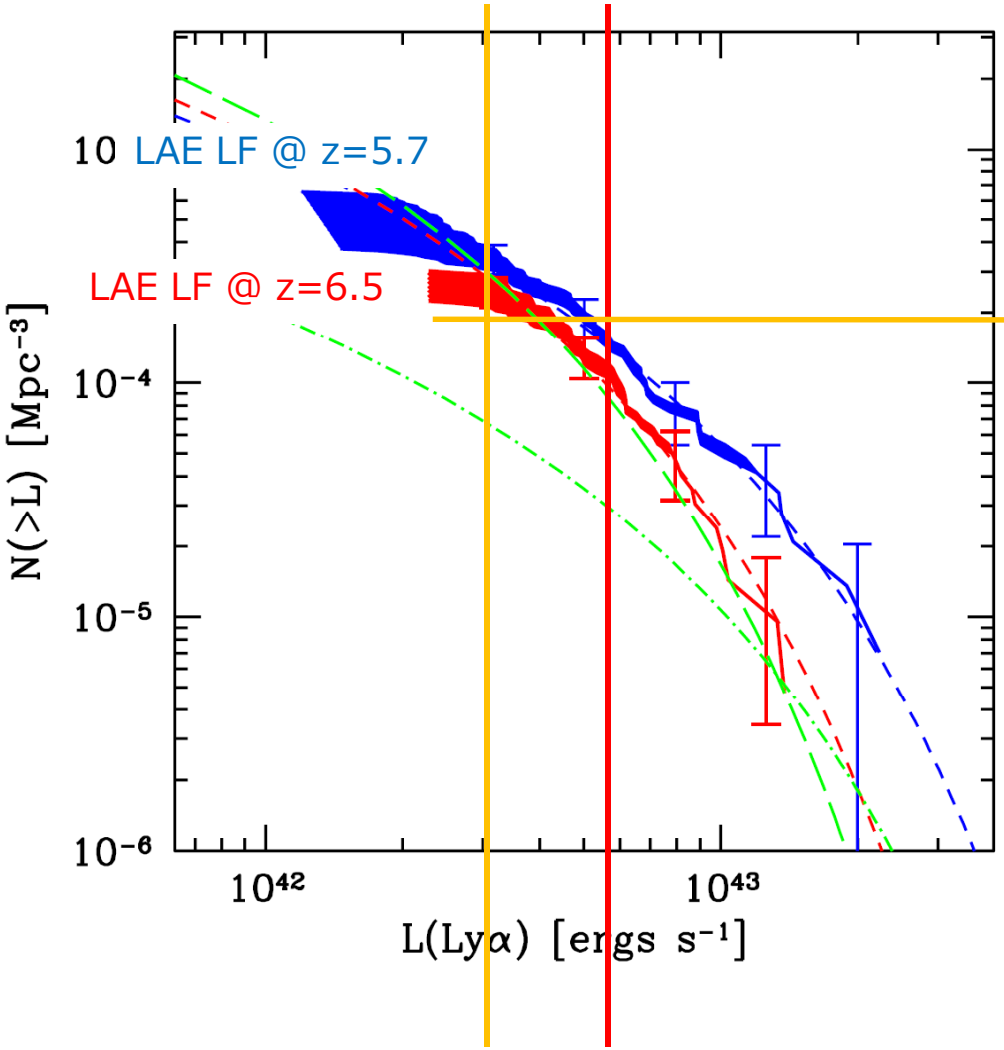

@z=7.7 @z=10.0

Subaru GLAO+WFI 10h limit

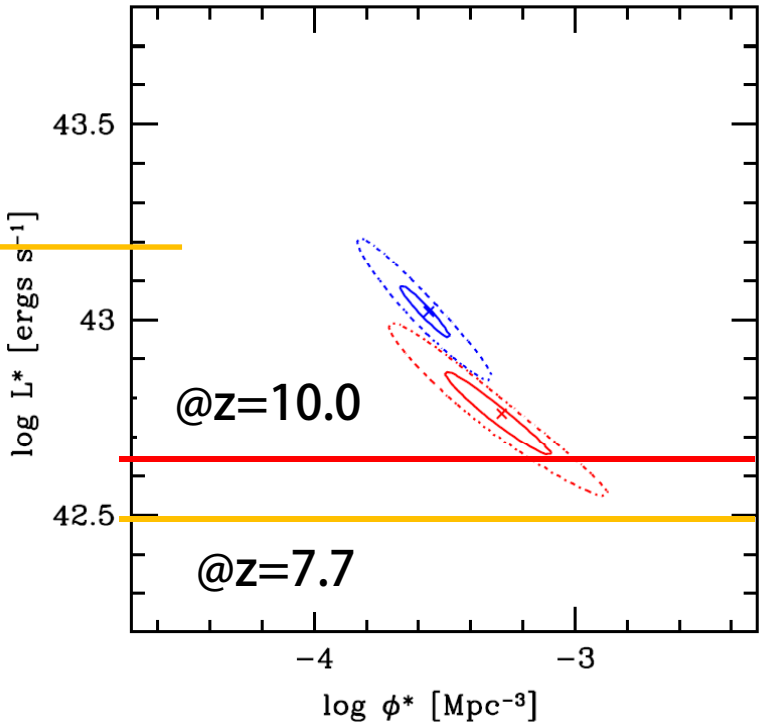

Kashikawa et al. 2010

Expected number of detections

Cases of No Evolution from z=6.5 LF by Kashikawa+2011
Maximum number

	10 hours x 3 fields		30 hours x 1 field		10 hours
	GLAO	Seeing	GLAO	Seeing	JWST
z=7.7	25.5	9.1	28.6	11.6	2.7
z=10.0	9.2	3.0	11.6	4.7	2x10^-4
z=11.8	7x10^-5	6x10^-7	2x10^-3	1x10^-4	0.3*

*** JWST/NIRCam. Z=7.7 and 10.0 are for NIRISS.**

Expected number of detections

Based on Semi-Analytic Model by Kobayashi et al. (cf. Kobayashi+2007; 2010)

	10 hours x 3 fields		30 hours x 1 field		10 hours
	GLAO	Seeing	GLAO	Seeing	JWST
z=7.7	12.2	7.6	6.27	4.83	--
z=10.0	1.5	0.6	2.2	0.7	--
z=11.8	0	0	0	0	0.003

Observation strategy with GLAO / Subaru

Still needs to consider,

Which is the best strategy : wide-shallow vs. narrow-deep ?

- It depends on the shape of Lyα LF.

What is the best narrow-band width and wavelength ?

- Good targets for TMT follow-up ?

How to obtain continuum image data ?

# S/N=10	# aprad	10h	30h	50h
z	GLAO	0.250	27.55	28.15	28.43
y	GLAO	0.250	26.65	27.24	27.52
J	GLAO	0.250	26.25	26.85	27.13

Filter width vs. line detection limit

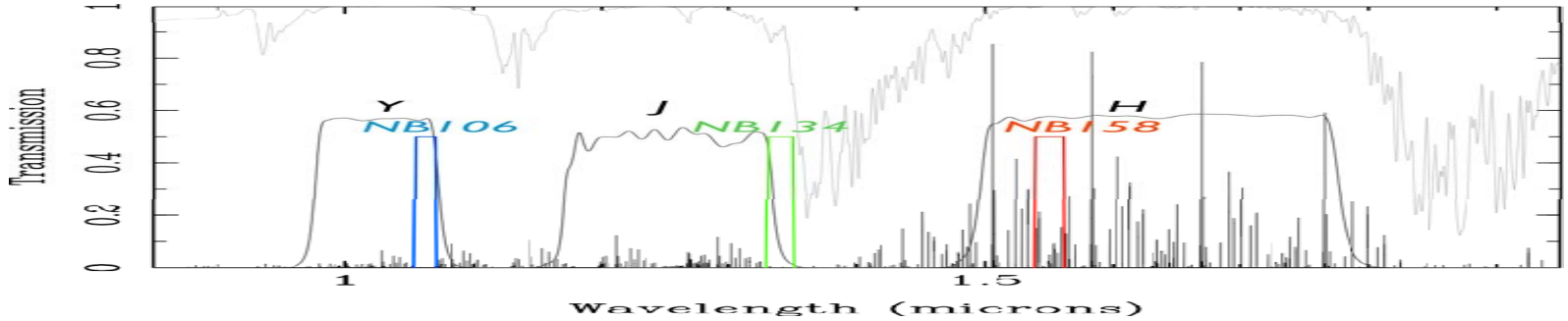

Relative detection limit (in mag. Unit) for line emission with constant SN with different filter width of Black : 3A, Red : 10A, Green : 30A, Blue : 100A, Cyan : 300A, Purple : 1000A ~ Broad-band. Line emission is assumed to be narrower than 3A. With the above assumption, narrower filters can achieve deeper detection limit.

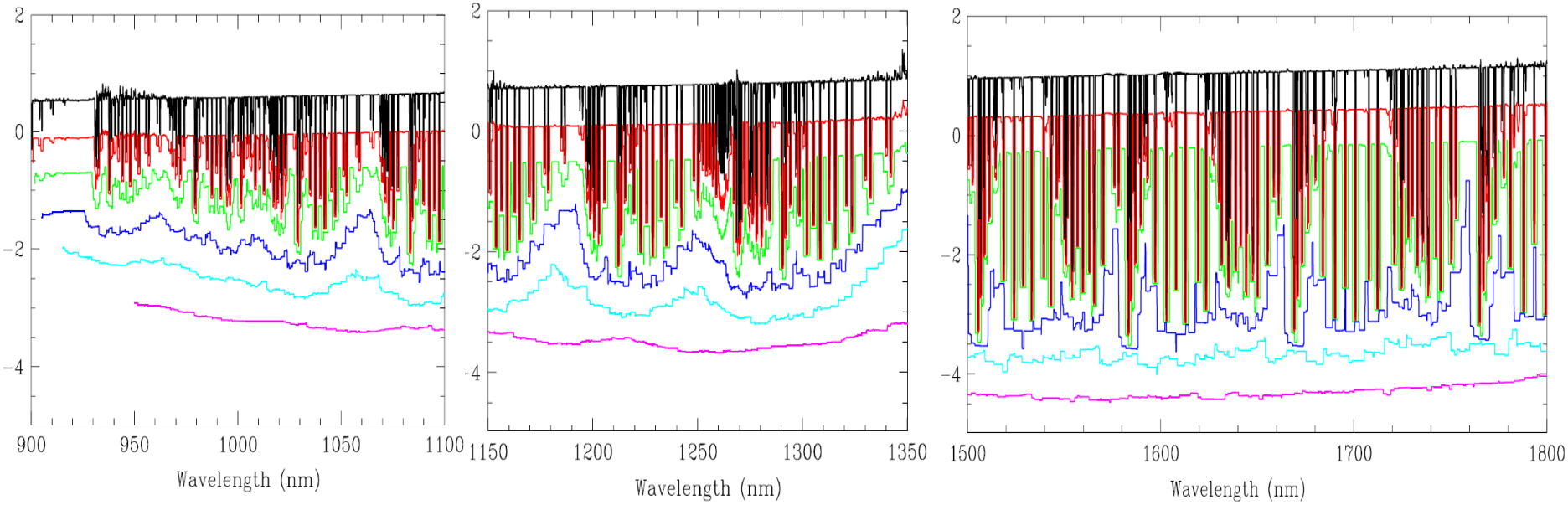

Filter width vs. LAE expected number

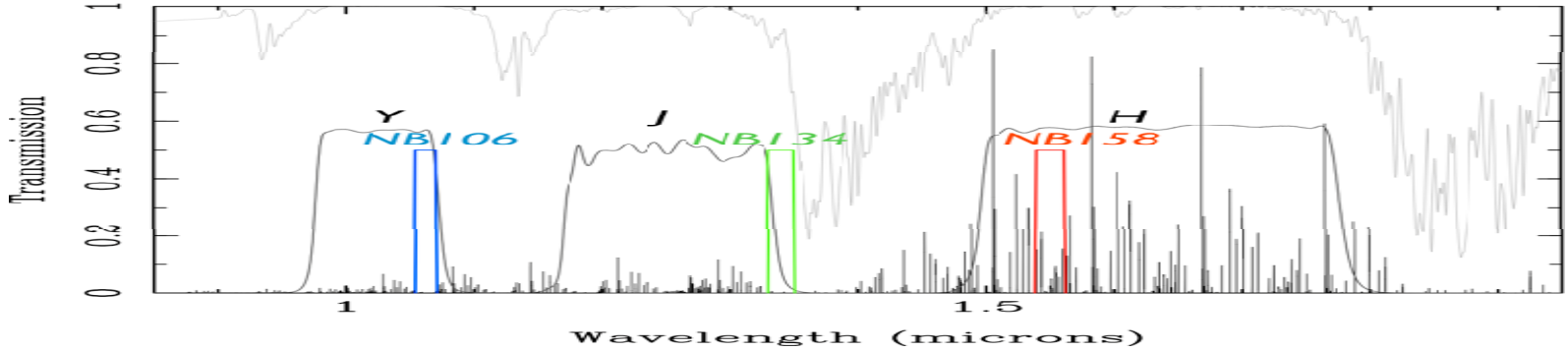

Relative expected number of emission line detection Black : 3A, Red : 10A, Green : 30A, Blue : 100A, Cyan : 300A, Purple : 1000A ~ Broad-band. The number density of emitters is assumed to be proportional to their line luminosity. ~30A width filter can achieve as good as narrower filters, but 100A width filter is good only in several limited bands.

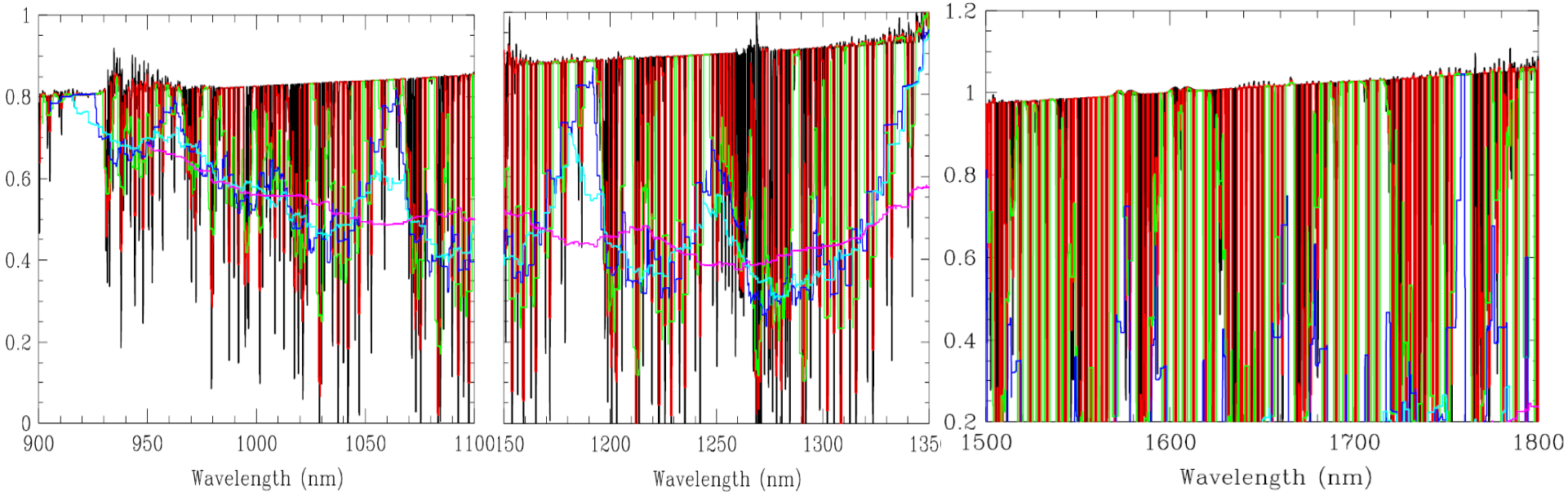

Filter width vs. LAE expected number

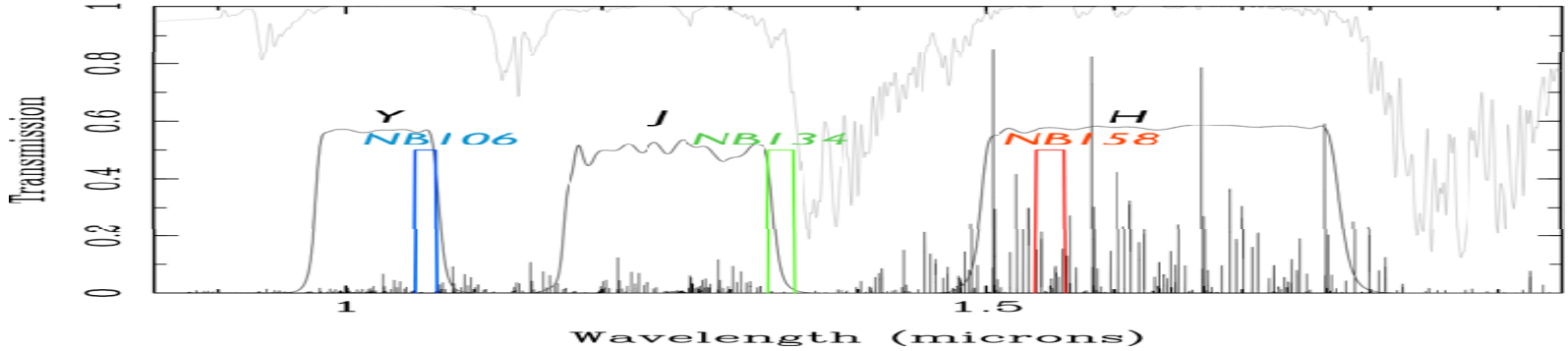

Relative expected number of emission line detection Black : 3A, Red : 10A, Green : 30A, Blue : 100A, Cyan : 300A, Purple : 1000A ~ Broad-band. The number density of emitters is assumed to be proportional to their line luminosity. ~30A width filter can achieve as good as narrower filters, but 100A width filter is good only in several limited bands.

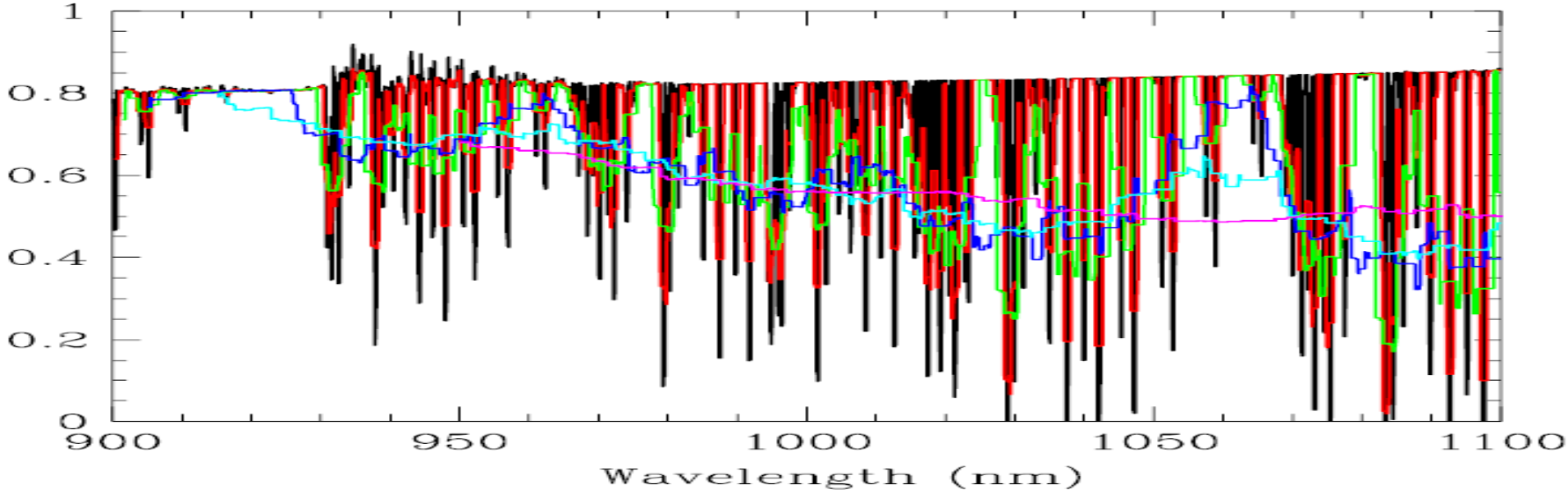

Filter width vs. LAE expected number

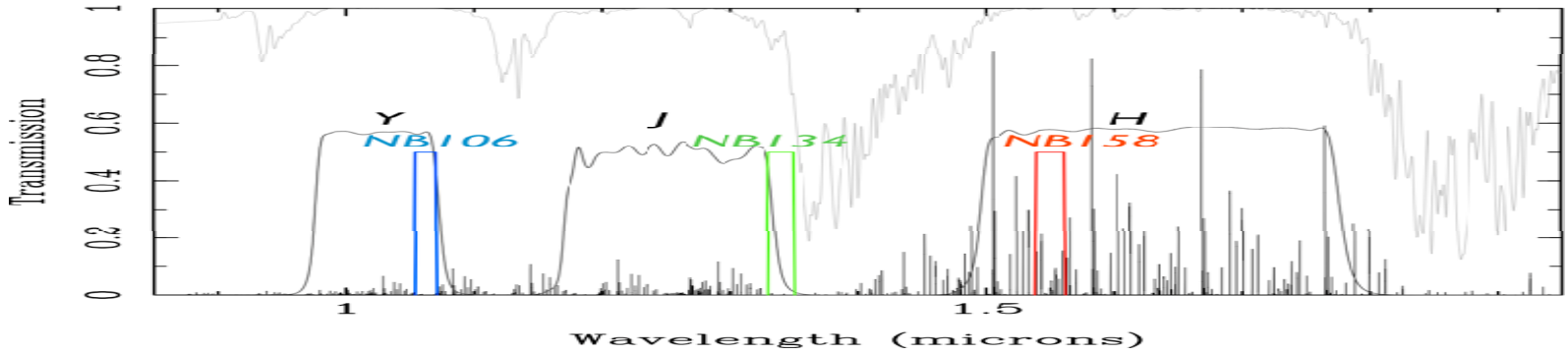

Relative expected number of emission line detection Black : 3A, Red : 10A, Green : 30A, Blue : 100A, Cyan : 300A, Purple : 1000A ~ Broad-band. The number density of emitters is assumed to be proportional to their line luminosity. ~30A width filter can achieve as good as narrower filters, but 100A width filter is good only in several limited bands.

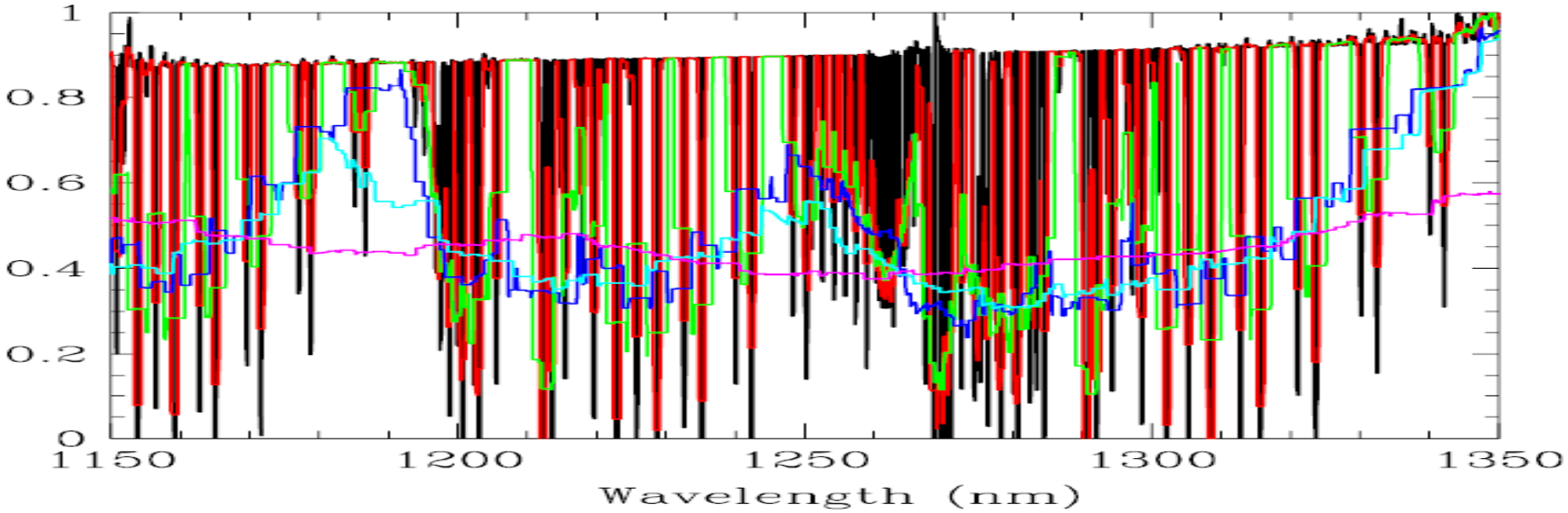

Filter width vs. continuum detection limit

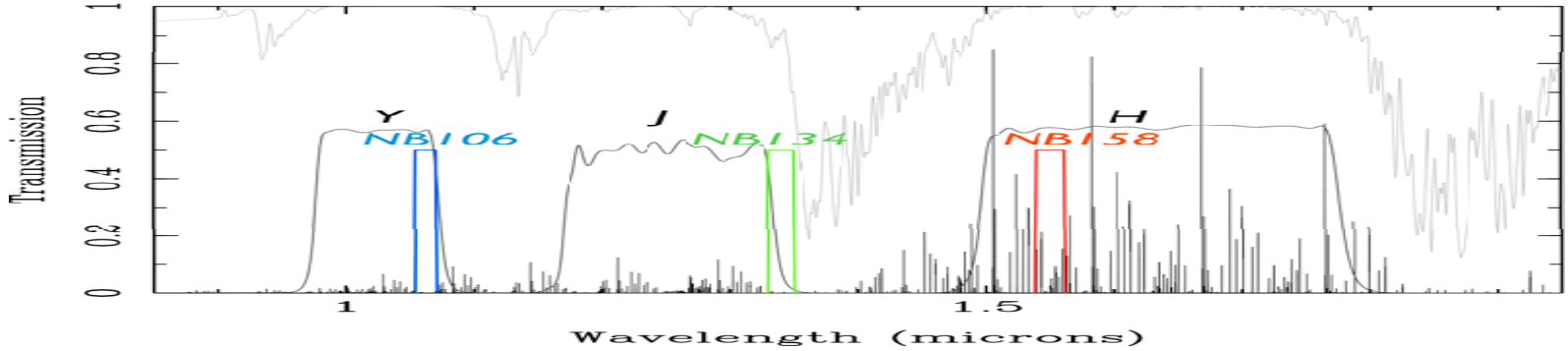

Relative detection limit (in mag. Unit) for continuum emission with constant SN with different filter width of Black : 3A, Red : 10A, Green : 30A, Blue : 100A, Cyan : 300A, Purple : 1000A ~ Broad-band. Continuum emission is assumed to have constant AB mag.

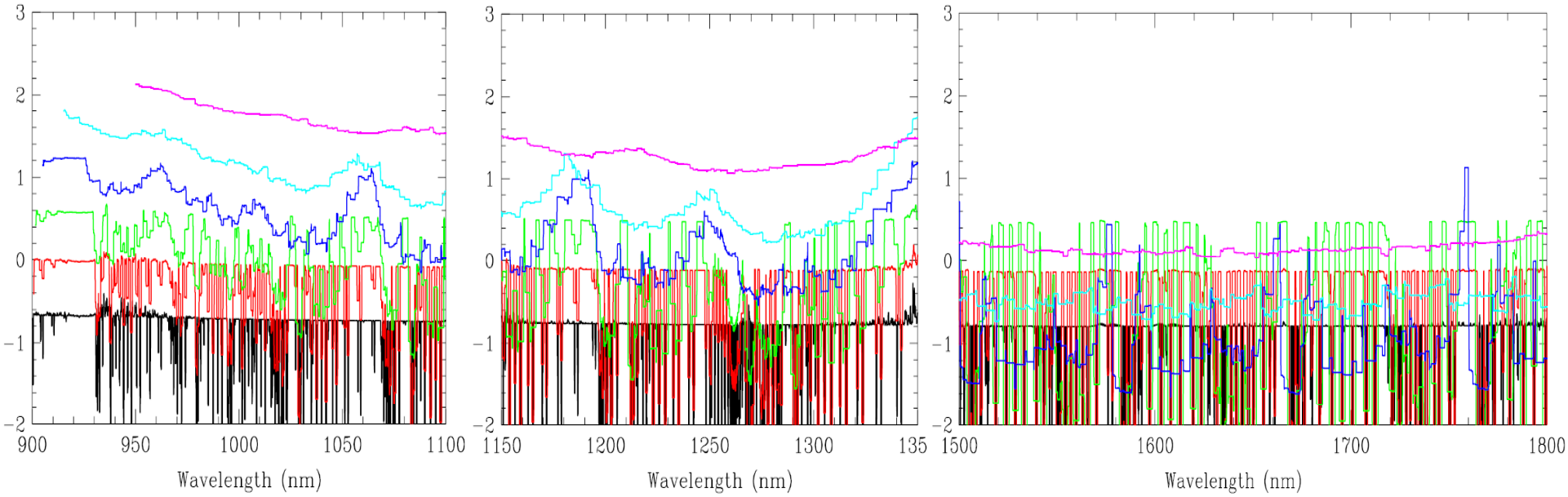

Summary / Answers

Q1: Wide-Field Near-IR Imager with NB capability (~30A width, possible ?)

Q2: Widest FoV is the best. Place scale is sufficiently high even with 0.10" sampling.

Q0: Do you need wide field near-IR imaging capability in the northern hemisphere after UKIRT ?

New idea after the talk:

How about combine narrow-band imaging data to make OH suppressed broad-band images ??

Additional Slide : TMT vs. JWST

Point source

(=photometric aperture
2xFWHM or 2xD.L.)
TMT: AO w/ 0.005”/pix w/o 0.1”/pix
JWST: 0.03”/pix @ nir

imaging

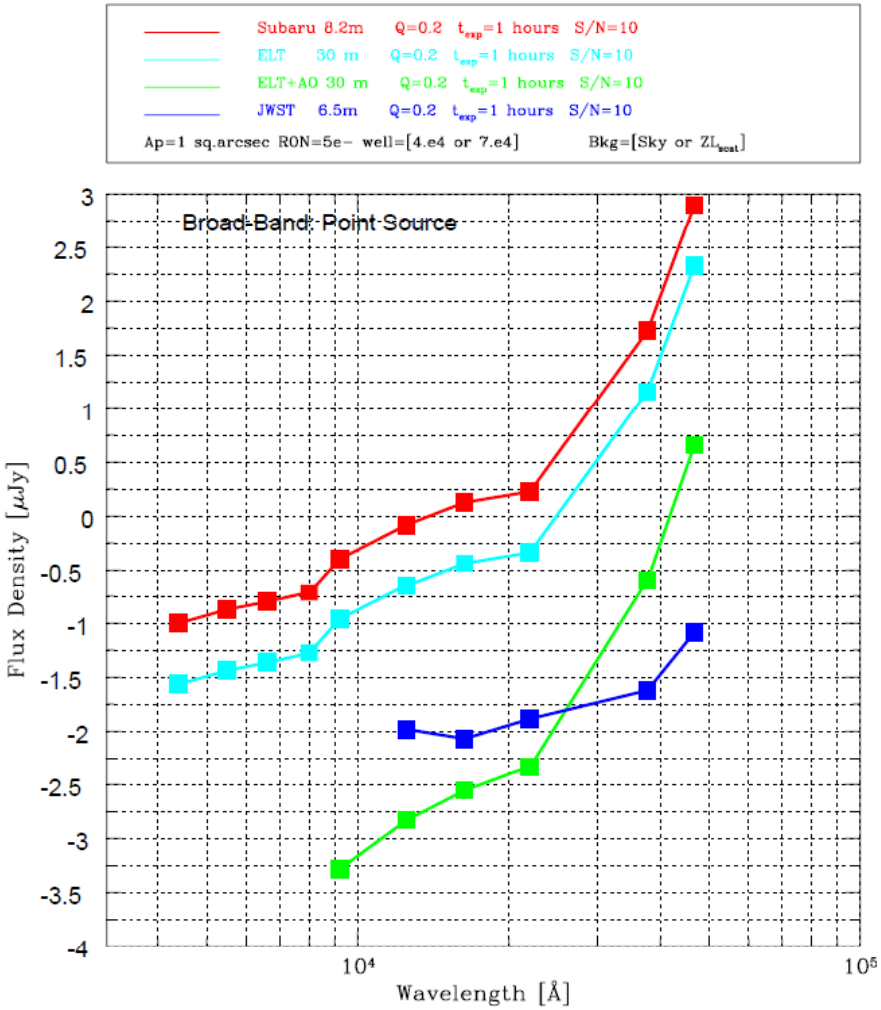

spectroscopy

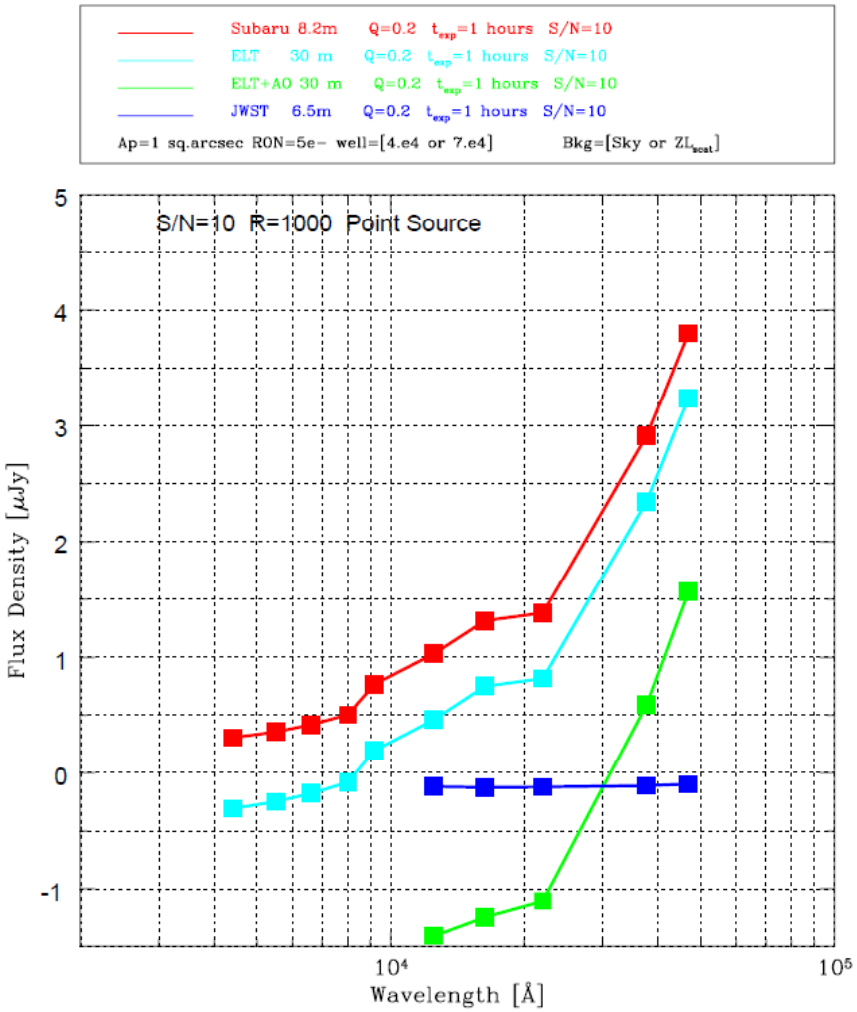

Extended source

(=photometric aperture 0.25 sq. arcsec.)
TMT: AO w/ 0.005”/pix w/o 0.1”/pix
JWST: 0.03”/pix @ nir

imaging

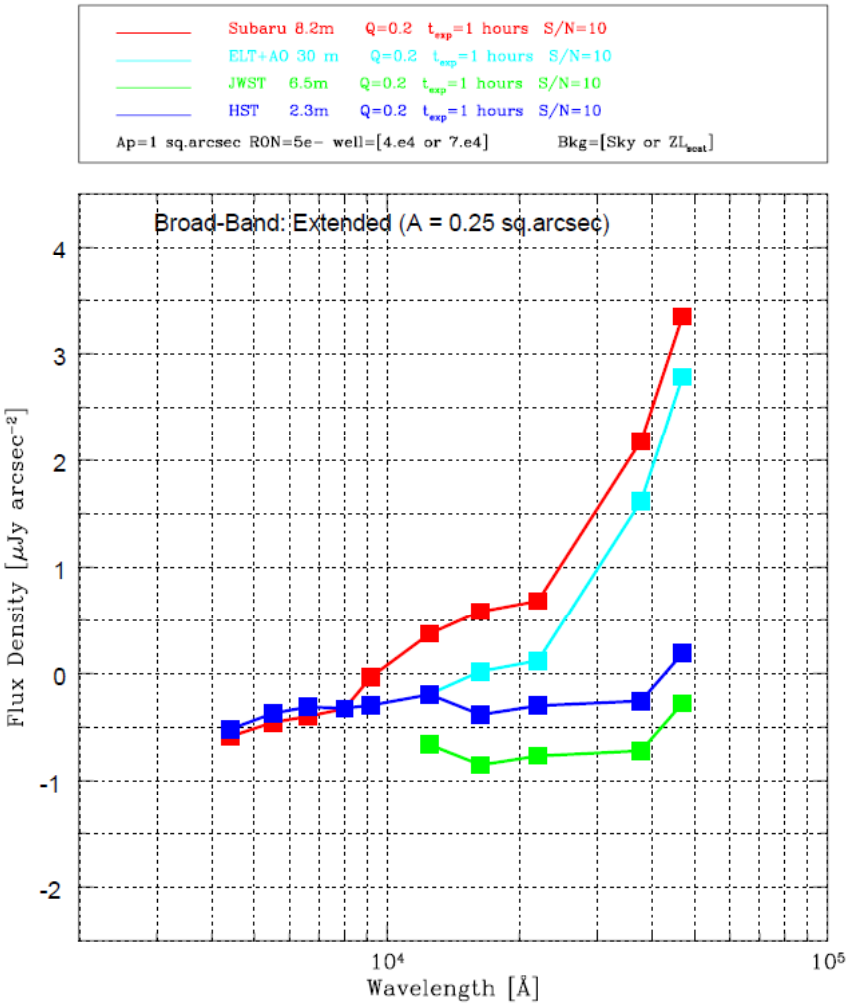

Spectroscopy (averaged over ~0.1nm)

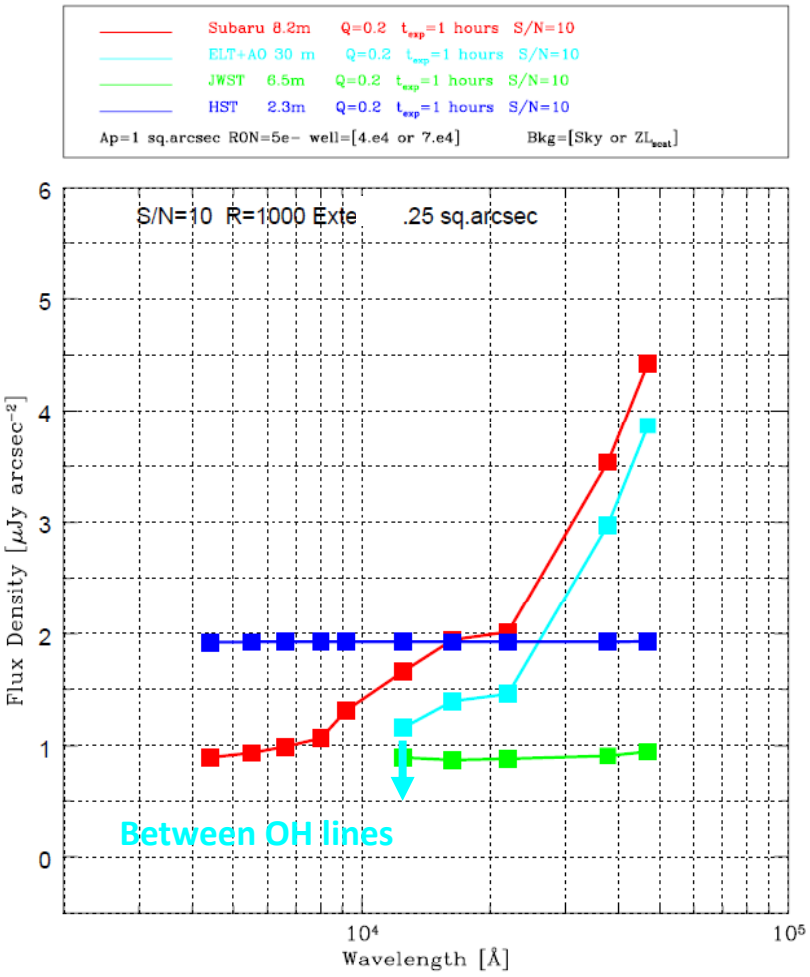

ELT w/ AO .. pixel sampling remained

Extended source

w/ and w/o AO fo TMT

imaging

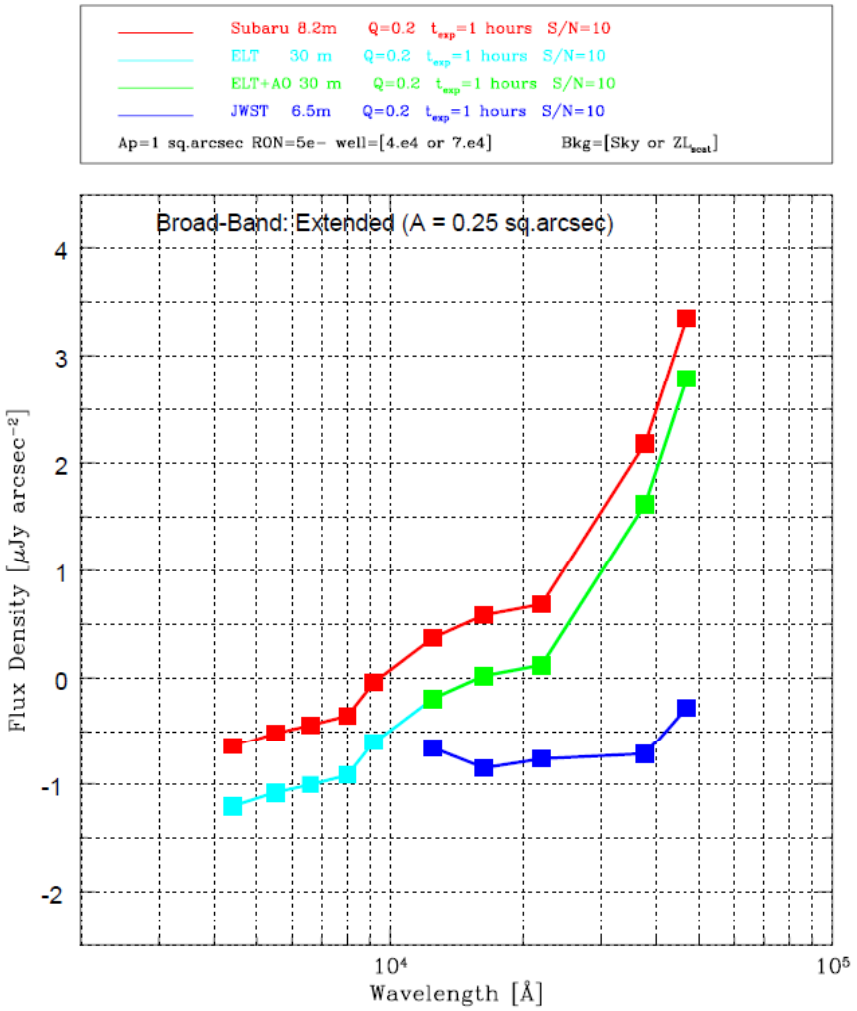

Spectroscopy (averaged over ~0.1nm)

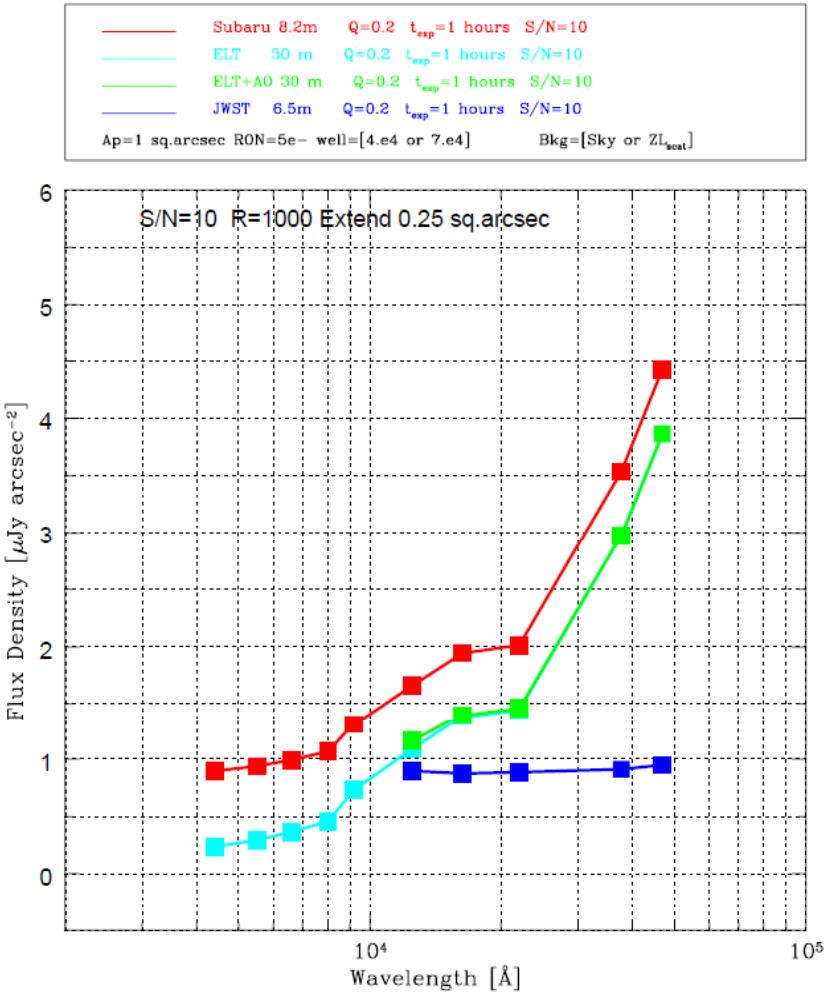

NIRCam Design Features

U of Arizona (M. Rieke) plus Lockheed ATC

- NIRCam images the 0.6 to 5μm (1.7 - 5μm prime) range
  - Dichroic used to split range into short (0.6-2.3μm) and long (2.4-5μm) sections
  - Nyquist sampling at 2 and 4μm
  - 2.2 arc min x 4.4 arc min total field of view seen in two colors (40 MPixels)
  - Coronagraphic capability for both short and long wavelengths
- NIRCam is the wavefront sensor
  - Must be fully redundant
  - Dual filter/pupil wheels to accommodate WFS hardware
  - Pupil imaging lens to check optical alignment

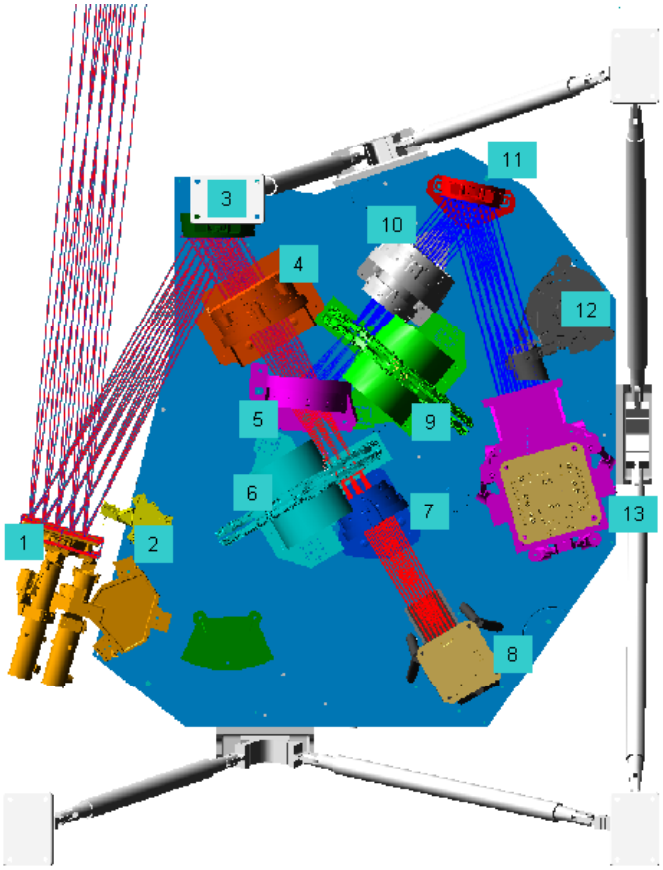

1	Pick-Off Mirror Assembly
2	Coronagraph
3	First Fold Mirror
4	Collimator Lens Triplet
5	Dichroic Beamsplitter
6	Long Wave Filter Wheel Assembly
7	Long Wave Camera Triplet
8	Long Wave Focal Plane Housing
9	Short Wave Filter Wheel Assembly
10	Short Wave Camera Triplet
11	Short Wave Fold Mirror
12	Pupil Imaging Lens
13	Short Wave Focal Plane Housing

NIRSpec

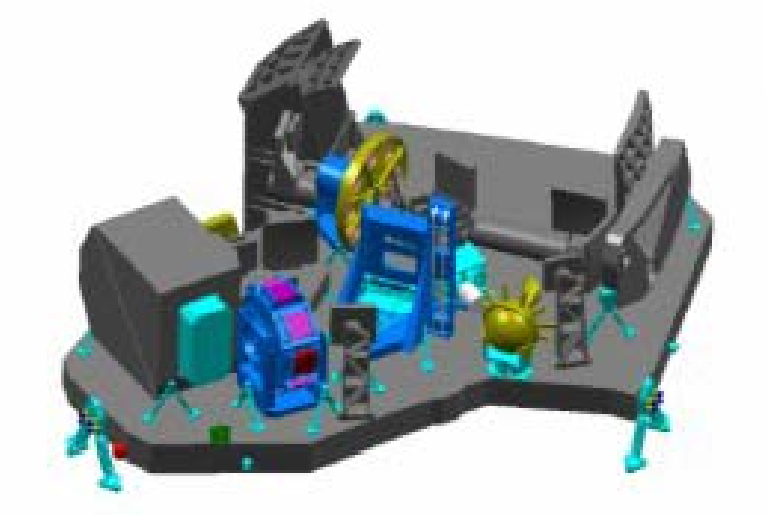

- Multi-object dispersive spectrograph (MOS) for 1-5 μm
- R~1000 or R~100 for MOS
- MOS pixels ~0.2", and cover a ~ ~3'x3' field
- Capable of observing > 100 objects simultaneously.
- Several fixed slits and an IFU (3"x3") are also available with R as high as 3000.
- Being built by the European Space Agency

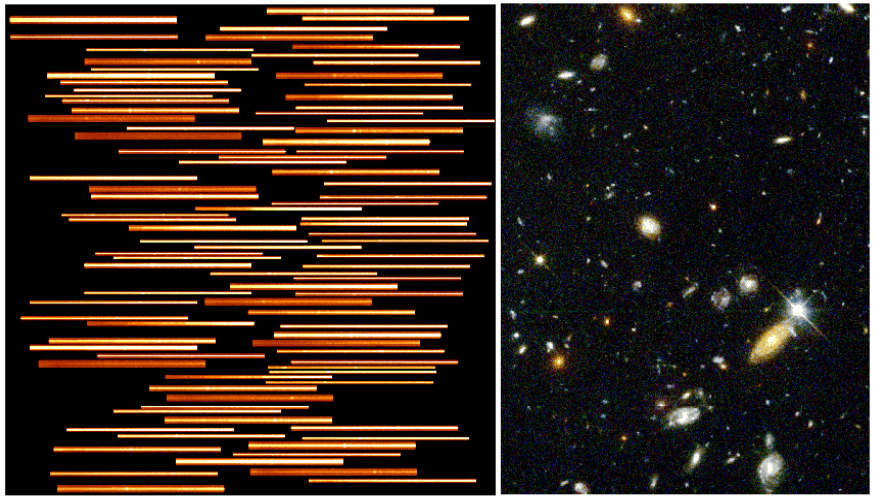

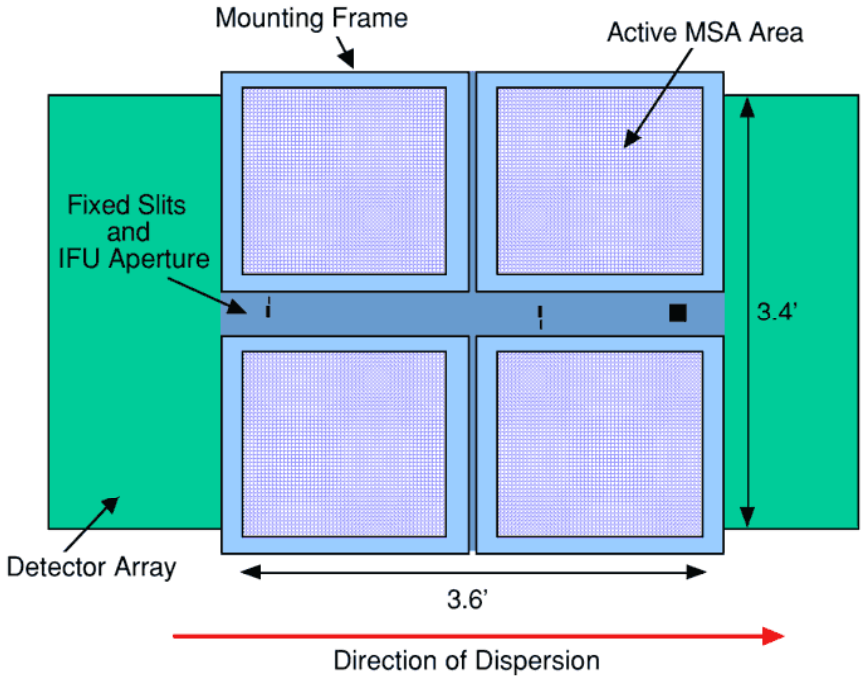

Another application of NB dataset

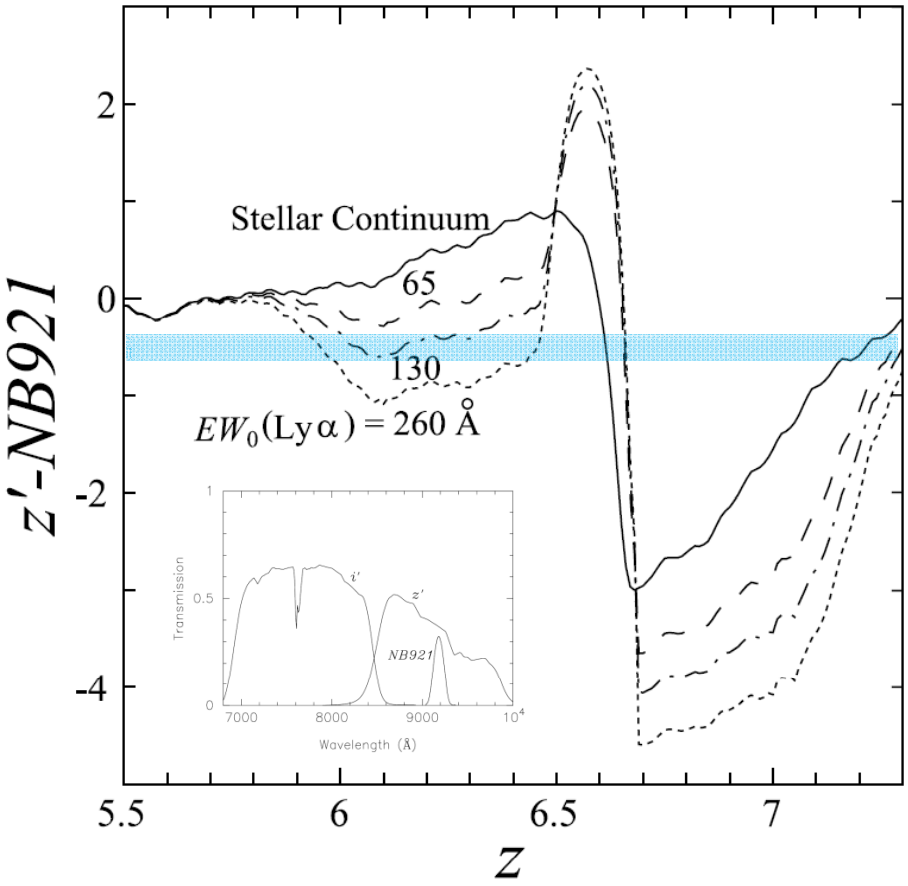

FIG. 5.—Expected $z' - \mathrm{NB921}$ color predicted by the stellar population synthesis model, as a function of redshift. The solid, dashed, dash-dotted, and dotted lines denote the stellar SED with Lyα whose rest-frame equivalent width is 0, 65, 130, and 260 Å, respectively.

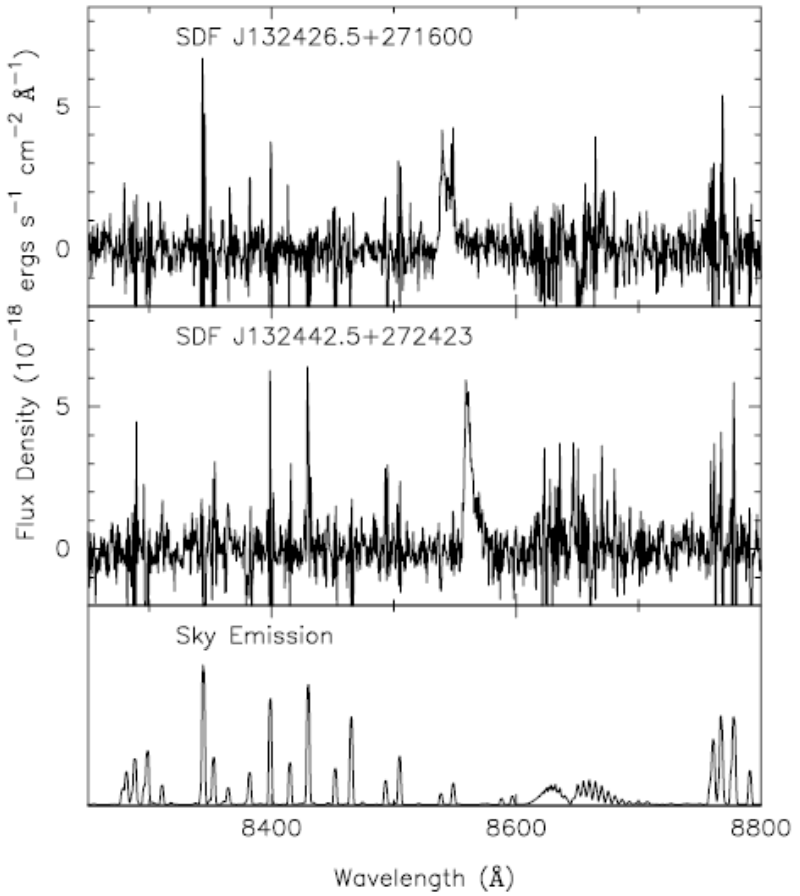

FIG. 3.—Optical spectra of SDF J132426.5+271600 (*top*), SDF J132442.5+272423 (*middle*), and typical sky emission (*bottom*).

Nagao et al. 2005, ApJ, 634, 142

EFFECT OF IGM

Effect of IGM on LAE detection: absorption and scattering

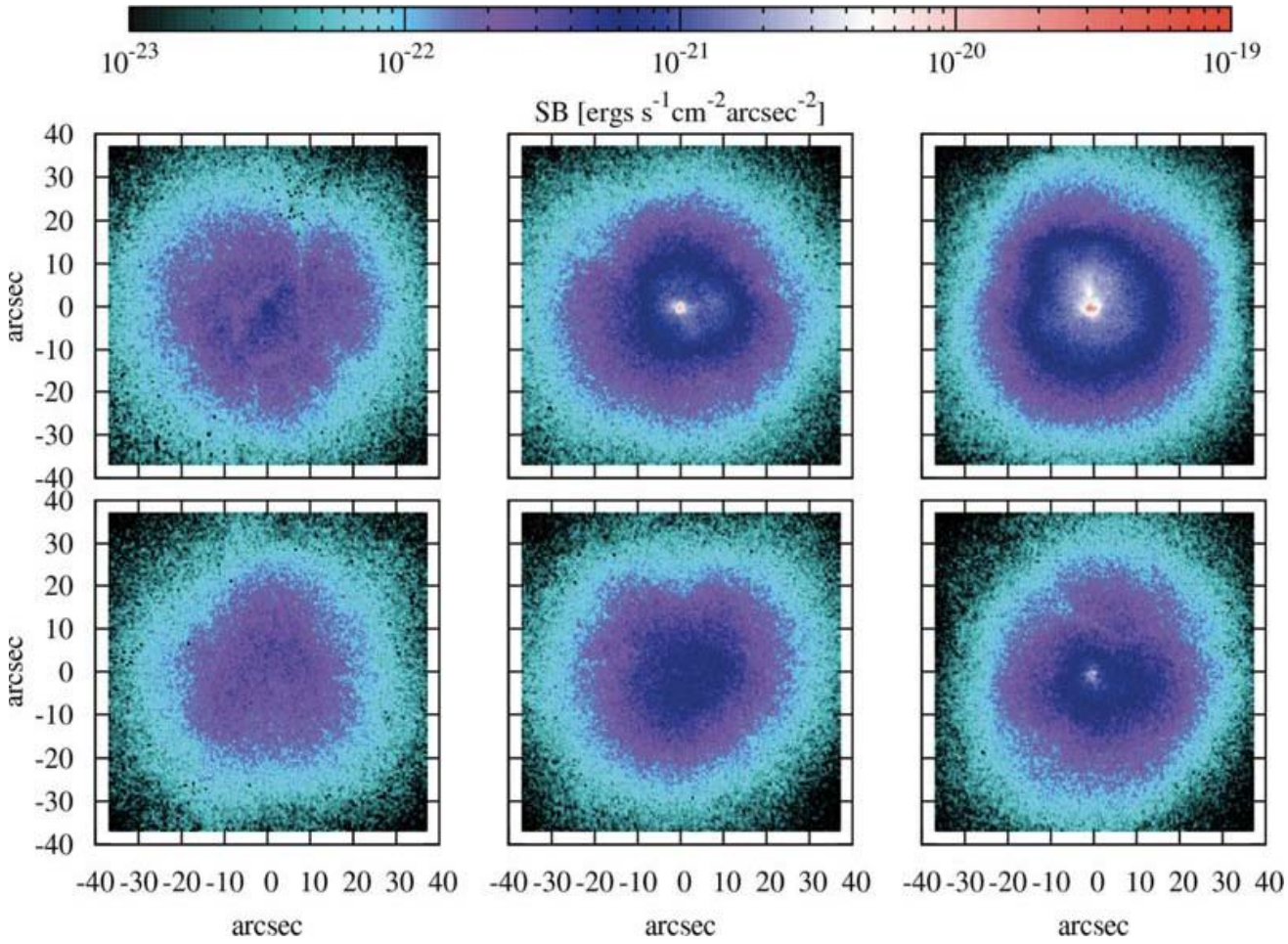

SPH+RT simulation: surface brightness from different angles

Jeeson-Daniel et al. 2012, MN 424, 2193

Expected LAE number counts depend on ionization fraction and surface brightness limits

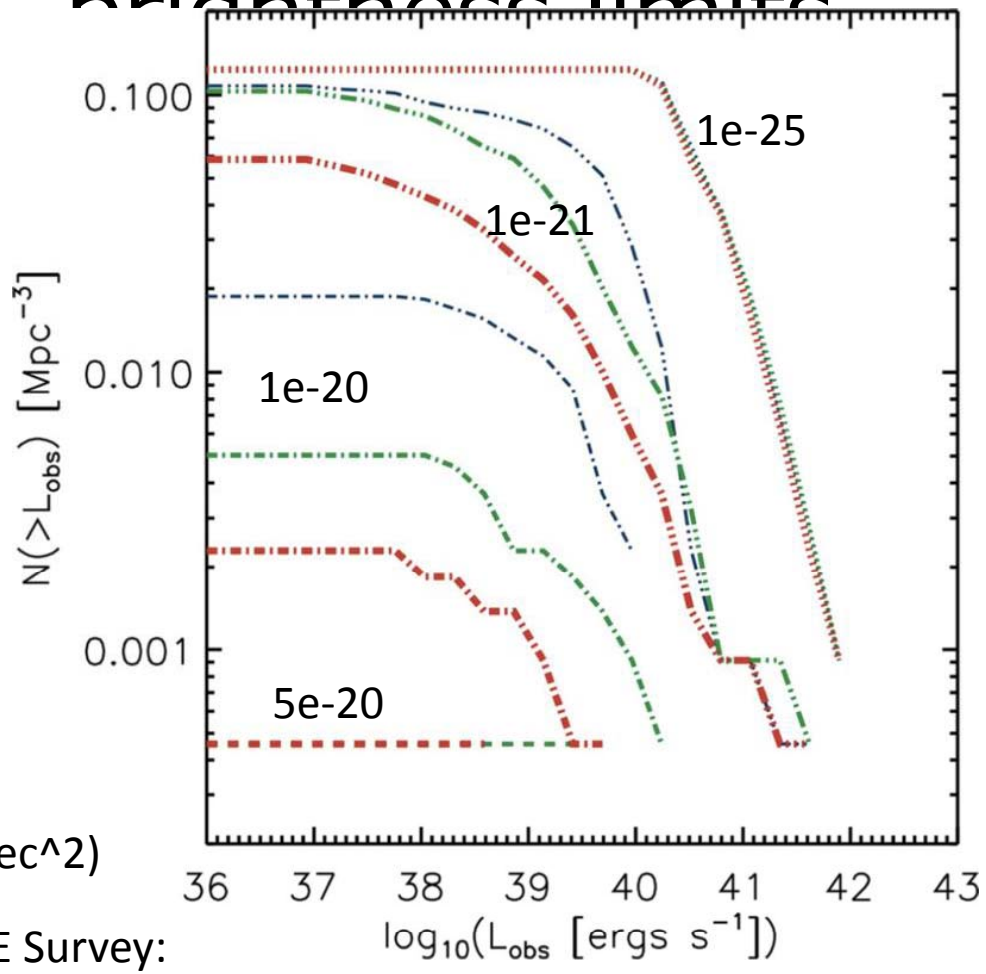

Red: x_ion=0
Green: x_ion=0.5
Blue: x_ion=0.89

Different lines:
SB cuts (erg/s/cm^2/arcsec^2)

Cf. Subaru SXDS z=5.7 LAE Survey:
2.64e-18 erg/s/cm^2/arcsec^2

Jeeson-Daniel et al. 2012, MN 424, 2193

Competition with JWST?

- JWST NIRCam does not have NBF $\lambda < 1.6\,\mu$m
- JWST NIRISS: R~150 Slitless spectroscopy with 2.2'x2.2' FoV

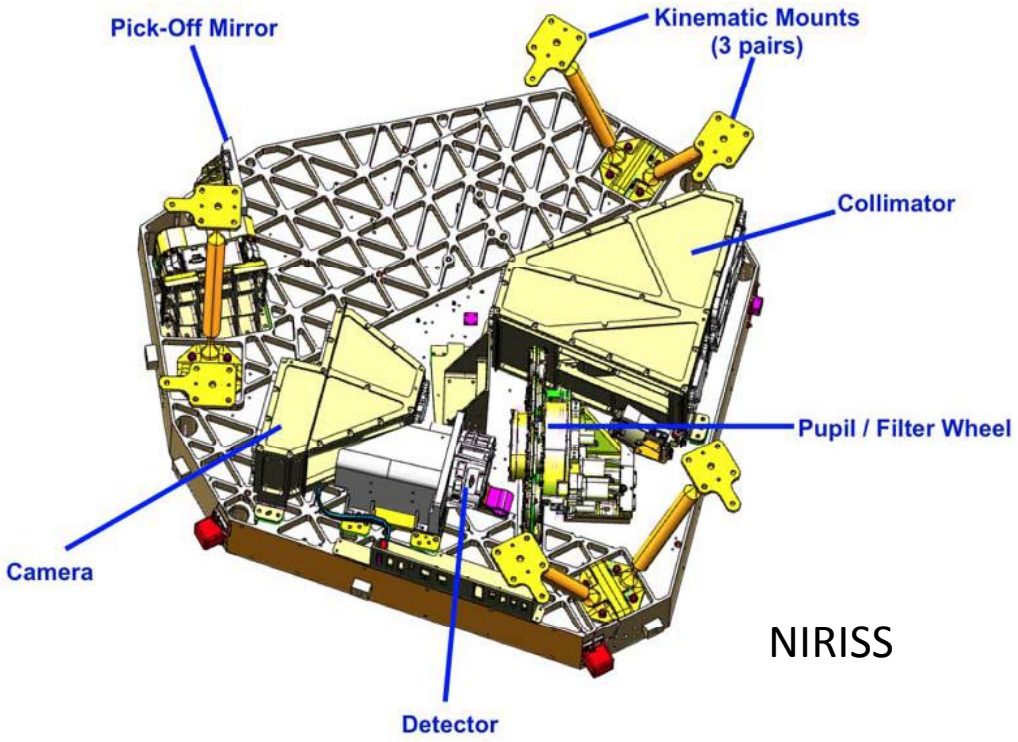

NIRISS

NIRCam filters

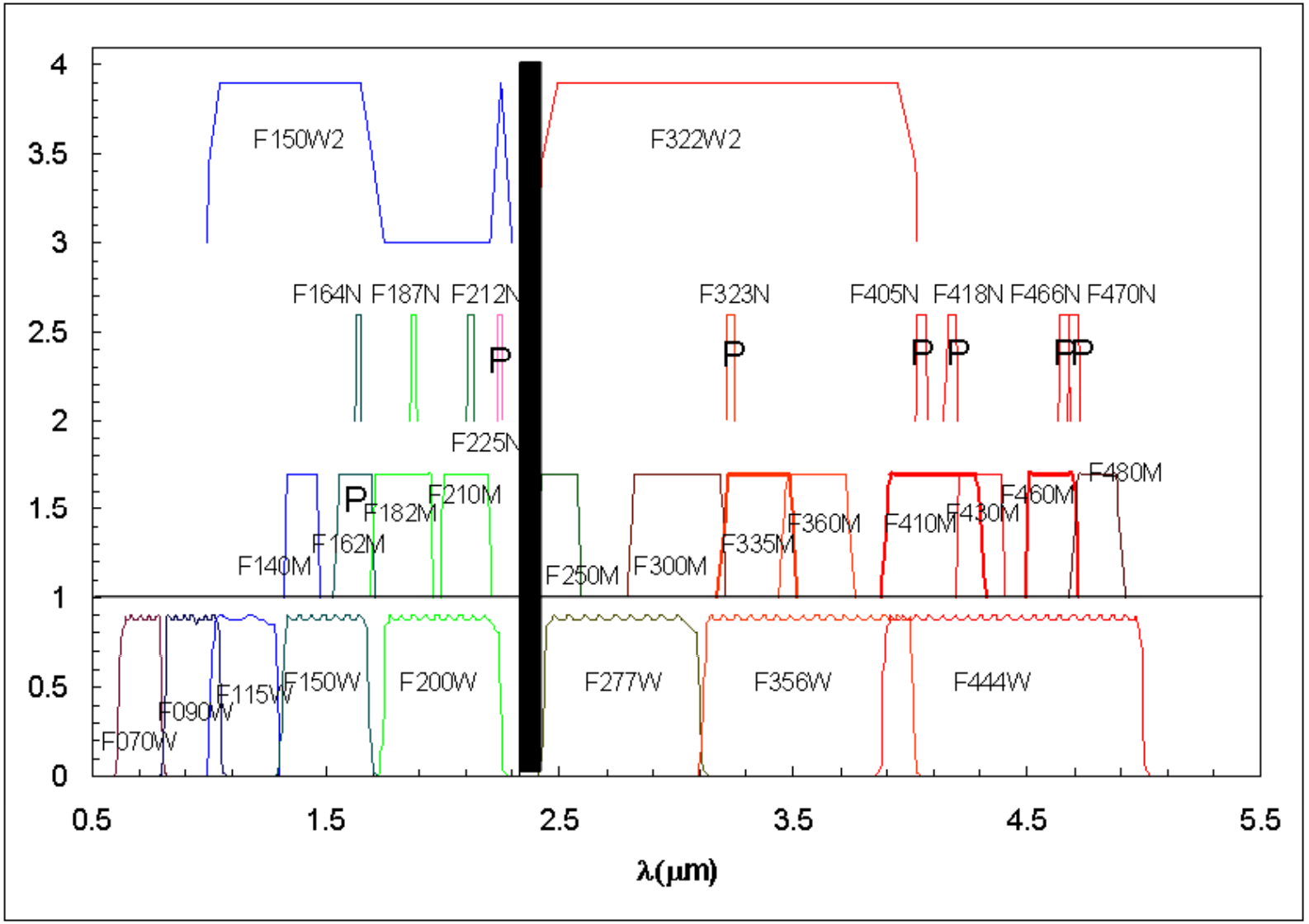

NIRISS slitless spec. sensitivity

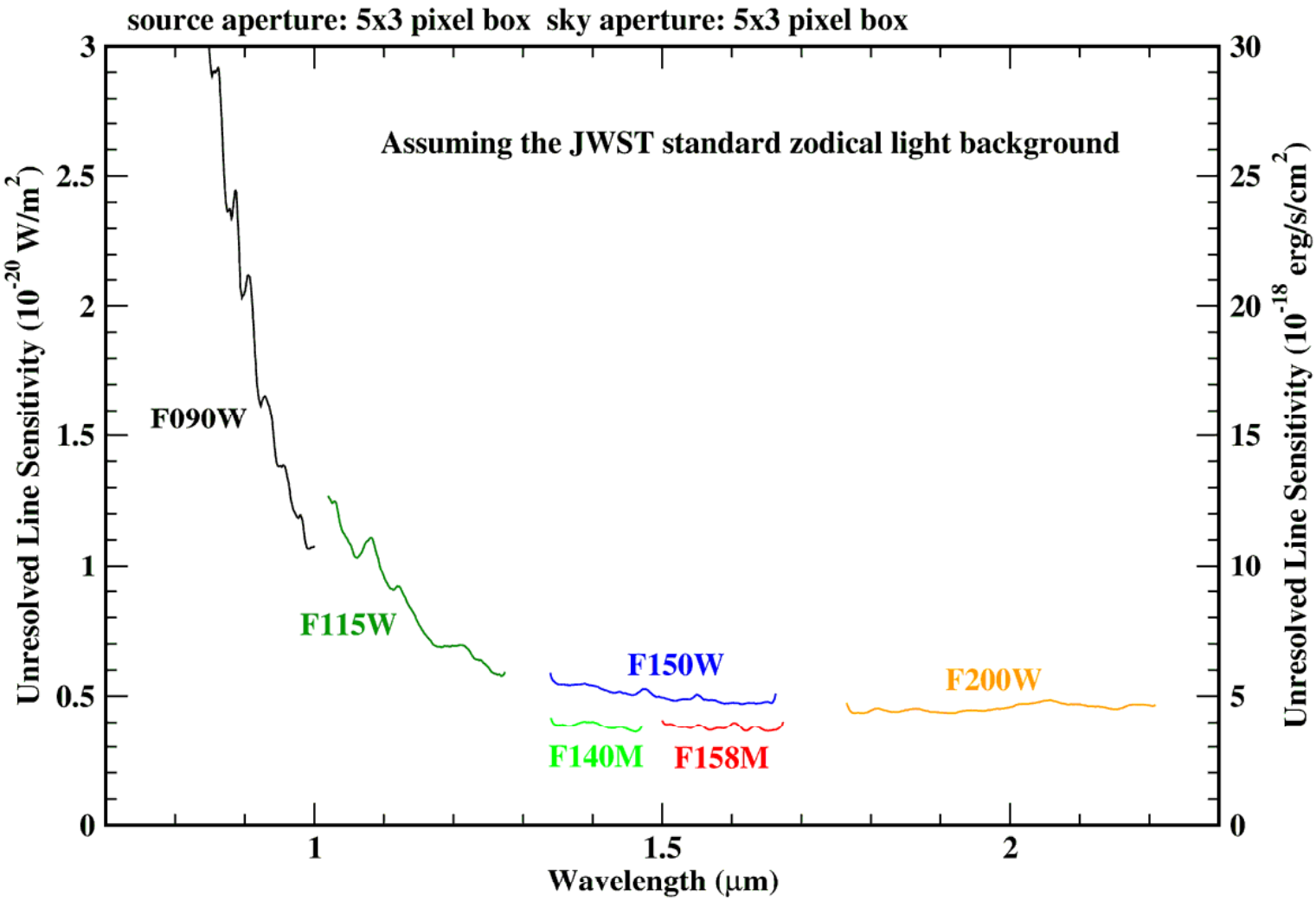

10^4 sec., S/N=10

2.6x10^-18 erg/s/cm^2 for S/N=5, 10 hours